



HAL
open science

Modeling Granular Materials: Century-Long Research across Scales

Farhang Radjai, Jean-Noël Roux, Ali Daouadji

► **To cite this version:**

Farhang Radjai, Jean-Noël Roux, Ali Daouadji. Modeling Granular Materials: Century-Long Research across Scales. *Journal of Engineering Mechanics - ASCE*, 2017, 143 (4), 10.1061/(ASCE)EM.1943-7889.0001196 . hal-01699485

HAL Id: hal-01699485

<https://hal.science/hal-01699485>

Submitted on 2 Feb 2018

HAL is a multi-disciplinary open access archive for the deposit and dissemination of scientific research documents, whether they are published or not. The documents may come from teaching and research institutions in France or abroad, or from public or private research centers.

L'archive ouverte pluridisciplinaire **HAL**, est destinée au dépôt et à la diffusion de documents scientifiques de niveau recherche, publiés ou non, émanant des établissements d'enseignement et de recherche français ou étrangers, des laboratoires publics ou privés.

MODELING GRANULAR MATERIALS: CENTURY-LONG RESEARCH ACROSS SCALES

Farhang Radjai¹

Jean-Noël Roux²

Ali Daouadji³

ABSTRACT

Granular materials are the most recurrent form of solid-state matter on Earth. They challenge researchers and engineers in various fields not only because they occur with a broad variety of grain sizes, shapes and interactions in nature and industry, but also because they show a rich panoply of mechanical states. Despite this polymorphism, all these different types of soils, powders, granules, ores, pharmaceutical products, ... are instances of the *granular matter* with the same least common denominator of being *sandlike* (psammoid in Greek), i.e. solid grains interacting via frictional contacts. This review describes milestone contributions to the field of granular materials since the early elastic-plastic models developed for soils in the 1950s. The research on granular materials has grown into a vast multi-disciplinary field in the 1980s with increasing focus on the microstructure and owing to new experimental tools and discrete simulation methods. It turns out that the granular texture, particle-scale kinematics and force transmission are far more complex than presumed in early micromechanical models of granular materials. Hence, constitutive relations cannot easily be derived from the particle-scale behavior although advanced continuum models have been developed to account for anisotropy, intermediate stress and complex loading paths. The subtle elastic properties and origins of bulk friction will be discussed, as well as the effects of particle shape and size distribution. The review covers also recent developments in macroscopic modeling such as the thermomechanical approach, anisotropic critical state theory, nonlocal modeling approach, inertial flows and material instabilities. Finally, a brief account is given of open issues and some new frontiers and challenges in the field.

Keywords: granular materials, constitutive modeling, micromechanics, multiscale modeling, thermomechanics, gradient plasticity, hypoplasticity, yield function, fabric tensor, flow rule, shear band, state parameter, non-associated flow rule, critical state theory, internal friction, dilatancy, force

27 chains, fabric tensor, nonaffine velocity, nonlocal model, jamming, entropy, second-order work,
28 discrete element method

29 **INTRODUCTION: AN OVERVIEW**

30 Granular matter has been a source of inspiration as much to little builders of sand castles on
31 the beach as to philosophers and poets who have been seeking in grains a window opening to the
32 invisible secrets of matter and life. “To See a World in a Grain of Sand . . .”, wrote William Blake.
33 Modern physics tells us that, depending on the resolution of measurement devices, a single grain
34 contains almost all about the laws of nature at increasingly smaller scales. But at larger scales,
35 those grains hold also the secrets of granular matter. Dissipative interactions among grains give rise
36 to an extraordinarily rich and complex bulk behavior of an assembly of grains. Eminent figures of
37 science and engineering were deeply concerned about odd behaviors arising from those interactions.
38 The unique properties of friction between two solid grains and its consequence for the stability of
39 a granular talus were introduced by Charles Coulomb (Coulomb 1773; Coulomb 1781). Dilatancy
40 (volume change under shear), discovered by Osborne Reynolds, appeared as much counterintuitive
41 as friction (Reynolds 1885). Memory effects, or “historical element” as put by James Maxwell,
42 were also recognized as a distinguishing feature of granular materials (Darwin 1883). The grains
43 can move like molecules in a gas but they dissipate energy by inelastic collisions and can get
44 “jammed” in a variety of configurations allowed by friction between grains and the action of their
45 weights or a confining stress. Terzaghi was intrigued by the variability of soils under different
46 loading conditions and the quasi-impossibility of arriving at the same level of scientific reliability
47 as in other materials (Terzaghi 1943). In a similar vein, as a result of energy dissipation at the
48 grain scale, granular materials do not seem to fit the general principles upon which the statistical
49 mechanics and thermodynamics of molecular fluids and solids were built (Jaeger and Nagel 1996).

50 There can be no comprehensive review of research on all aspects of granular matter in a single
51 paper – even when limited to cohesionless dry granular materials as in the present paper. Here, the
52 focus will be on those features that are believed to have strong bearing on the future developments in
53 this field. It should also be borne in mind that, despite many multidisciplinary workshops organized
54 for 30 years, there still remain high cultural barriers between various communities involved in
55 research on granular materials. The level of expectation from such a research and the ultimate

56 goals are often quite different. Our goal here is to contribute to cross fertilization among disciplines
57 by mainly emphasizing the guiding ideas and concepts and avoiding technical developments.

58 During the 20th century, two scientific communities were involved in modeling granular materi-
59 als: soil mechanics and powder technology. The Mohr-Coulomb plastic behavior is and remains at
60 the heart of soil mechanics which has been primarily interested in predicting soil failure whereas
61 powder technology has mostly been concerned with large deformations and continuous flow of
62 granular materials often regarded as a suspension. In the 10th Rankine Lecture in 1970, Roscoe
63 emphasized the need to understand the stress-strain behavior of soils well before failure under
64 complex loading conditions as encountered in engineering practice (Roscoe 1970). Fully aware of
65 the need for a fundamental approach, he indicated the route towards a fundamental understanding
66 of soils by working “with soils in their simplest possible states (e.g. well graded sands and satu-
67 rated remolded clays) so that their properties can be defined by the minimum possible number of
68 parameters”, preparing “soil samples in initially uniform states”, developing test equipments and
69 “non-destructive methods of checking the uniformity of the behavior of the soils at all stages of
70 these tests” and developing “scanning electron microscopy methods of studying the change of soil
71 fabric during mechanical deformation”. This is the route which was followed during the coming
72 decades.

73 A consistent model of soil plasticity was actually achieved through the “critical-state soil me-
74 chanics” of the Cambridge School (Roscoe et al. 1958; Schofield and Wroth 1968; Wood 1990). By
75 accounting for both frictional and volume-change behaviors of soils and, more importantly, by rec-
76 ognizing a family of memoryless states reached after long enough shearing, it provided for the first
77 time a general framework for the quasi-static behavior of both clays and granular soils. The critical
78 state theory is the core of nearly all constitutive models that were developed later to account for
79 complex loadings paths. Critical states are asymptotic states approached for large enough strains,
80 applied monotonically and quasistatically. Constitutive laws predicting this gradual approach are
81 traditionally elastoplastic in nature. The elastic properties of granular materials have been clari-
82 fied, over the past 25 years, thanks to improved experimental techniques apt to measure very small
83 strain intervals (Shibuya et al. 1992; Hicher 1996). Elastic waves (Goddard 1990a) are actually the
84 reflection of the quasistatic elastic behavior of small amplitude perturbations about an equilibrium
85 state of a solid granular assembly (Thomann and Hryciw 1990; Shibuya et al. 1992; Geoffroy et al.

86 2003). Due to nonlinear contact elasticity, their velocity depends on the stress level. While grain-
87 scale disorder induces incoherent propagation, larger wavelengths propagate coherently (Liu and
88 Nagel 1992; Liu 1994; Liu and Nagel 1994; Jia et al. 1999).

89 Micromechanical approaches to the plastic (Christoffersen et al. 1981; Bathurst and Rothenburg
90 1988; Chang and Misra 1990) and elastic (Walton 1987; La Ragione and Jenkins 2007) behaviors
91 of granular materials have been an active area from the outset of modern research on granular
92 materials. The onset of instabilities in granular materials as a function of the loading program has
93 also been a subject of extensive investigation under homogeneous boundary conditions (Vardoulakis
94 1979; Lade 1994; Vardoulakis and Sulem 1995; Nova 1994; Darve and Laouafa 1999; Lade 2002;
95 Nicot and Darve 2007; Chang et al. 2011). Directional loading reveals that material instability
96 can occur in a diffuse form or be localized in a shear band. Imaging techniques have been used to
97 analyze shear bands in which plastic deformations are fully developed (Desrues et al. 1983; Desrues
98 et al. 1996).

99 Besides quasi-static deformations, which may be coined as “Coulomb regime”, granular materi-
100 als can be found in at least two dynamic regimes depending on the time scales involved (Goddard
101 2014): 1) Inertial flows (Bagnold regime), and 2) granular gases. Stresses in dense inertial flows
102 have been known since Bagnold to scale quadratically with the shear rate (Bagnold 1954), but the
103 full scaling was more carefully analyzed only recently by introducing a dimensionless inertial num-
104 ber and applied to different flow geometries (inclined plane, tube, rotating drum, . . .) (GDR-MiDi
105 2004; da Cruz et al. 2005). This scaling indicates that the Coulomb friction angle can be extended
106 to the inertial regime, where energy is dissipated by both inelastic collisions and friction between
107 grains, and increases with inertial number. In the limit of high shear rates or vibration-induced
108 fluidization, long-lasting contacts disappear and the granular material turns into a gas governed
109 by collisions. Granular gases differ from molecular gases in requiring continuous energy input from
110 outside and, hence, they are never in statistical equilibrium (Walton and Braun 1986; McNamara
111 and Young 1992; Goldhirsch and Zanetti 1993; McNamara and Young 1994). Despite their local
112 inhomogeneities induced by inelastic collisions, they can be described by a kinetic theory in which
113 quadratic velocity fluctuations play the role of *granular temperature* (Jenkins and Richman 1985).
114 The thermodynamic temperature plays, by definition, no role in the dynamics of granular materials.
115 For this reason, the velocity fluctuations are basically controlled by energy input rate.

116 Alongside macroscopic testing and modeling approaches, photoelastic experiments of Dantu
117 (Dantu 1957) and careful measurements by Biarez (Biarez 1962) and Oda (Oda 1972) revealed
118 the highly inhomogeneous and anisotropic nature of granular materials at the grain scale under
119 shearing. Computer simulations by the Discrete Element Method (DEM), based on incremental in-
120 tegration of rigid grain displacements and rotations by accounting for frictional contact interactions
121 between grains, provided for the first time direct access to the full dynamics of grains and evolution
122 of granular fabric (Cundall and Strack 1979; Cundall and Strack 1983; Thornton and Randall 1988;
123 Bathurst and Rothenburg 1988; Moreau 1993). It was then believed that by including microstruc-
124 tural information, a macroscopic model of quasi-static behavior can soon be achieved with internal
125 variables fully based on the granular microstructure. However, packing properties induced by steric
126 exclusions between particles and geometrical disorder are complex and rich.

127 This was actually the point where the mechanics of granular materials joined the physics of
128 amorphous materials such as liquids and glasses in which the packing of hard grains plays a central
129 role (Bernal 1960; Berryman 1986; Pavlovitch et al. 1991; Jullien et al. 1992; Torquato 2010). The
130 concept of Random Close Packing (RCP) was revisited in this context, (O’Hern et al. 2003; Donev
131 et al. 2005; Agnolin and Roux 2007a; Peyneau and Roux 2008a) and that of jamming was intro-
132 duced (Berryman 1986; Cates et al. 1998; Liu and Nagel 1998) to characterize stability of equilibria
133 in which external forces are balanced by steric impenetrability constraints. Statistical characteri-
134 zations of granular microstructure have been pursued for 20 years in a multidisciplinary context.
135 Force distributions (Liu et al. 1995; Radjai et al. 1996; Mueth et al. 1998; Radjai et al. 1998),
136 nonaffine particle displacements (Radjai and Roux 2002; Combe et al. 2015), local rearrangements
137 and particle rotations (Kuhn 1999; Bardet 1994; Oda et al. 1997; Kuhn and Bagi 2004; Estrada
138 et al. 2008) and many other features have been carefully analyzed. A rigorous relation between
139 shear stress and fabric anisotropy was introduced by the partition of stress tensor (Bathurst and
140 Rothenburg 1988; Radjai and Richefeu 2009). But the relevant internal variables for the plastic
141 behavior of granular matter remain still open to current research.

142 Granular matter came vigorously to the focus of physics through a “sandpile” metaphor of
143 *self-organized criticality* (SOC) (Bak et al. 1987): A sandpile can be built by allowing grains to fall
144 successively into a substrate. As the pile grows, a steady state is eventually reached without tuning
145 any control parameter (self-organized) and with fluctuations (avalanches of grains on the surface

146 of the pile) distributed as a power law (criticality), reflecting the absence of intrinsic time and
147 length scales in this state, as in a second-order phase transition. Although a power-law distribution
148 of grain avalanches was not experimentally observed, the SOC brought to the light the highly
149 nonlinear behavior of granular materials and their phase transformations (from solid-like to liquid-
150 like) under moderate energy inputs or stress increments (Jaeger et al. 1990). That is how simple
151 sand was suddenly transformed into a paradigm of complexity, inviting researchers from various
152 fields to develop a fresh look at old real problems.

153 Most of research in the past thirty years has focussed on model granular materials. The fact that
154 simple spherical particles with frictional contacts produce nearly all complex behaviors of granular
155 materials, extends the status of simple packings as the core model of all granular materials. This is
156 all the more fortunate that the effects of numerous parameters describing real granular materials can
157 be characterized by comparison with this model. Assemblies of rigid, frictionless particles (Roux
158 2000; Combe and Roux 2000; Wyart et al. 2005; Peyneau and Roux 2008a) have also been studied
159 as extreme case models in which all mechanical response is determined by geometric constraints.
160 Going away from the simplest models, particle size distribution (PSD) is crucial for both space-
161 filling and shear properties of granular materials. Surprisingly, recent simulations seem to show
162 that the internal friction angle is not dependent on the PSD since force transmission is controlled
163 by the class of largest particles (Voivret et al. 2009).

164 The effect of particle shape has been more systematically investigated for a few years, and here
165 again the space-filling aspects are counterintuitive and the shear behavior and its relation with the
166 microstructure are complex (Donev et al. 2004; Azéma et al. 2007; Azéma et al. 2009; Torquato
167 2010; Katagiri et al. 2010; Nguyen et al. 2014; Jaeger 2015). The concept of *jamming transition* has
168 emerged in physics for unifying the rheology of granular materials with other amorphous materials
169 such as glasses, colloids and foams (Liu and Nagel 1998). Slight variations of temperature close to
170 such a transition lead to the increase of viscosity by orders of magnitudes in a supercooled liquid in
171 the same way as small variations of packing fraction in a granular material control transition from
172 a liquid-like to a solid-like state (Jaeger 2015). This emergence of shear strength is quite rich when
173 particles of strongly nonconvex shape are considered. By monitoring particle shape parameters and
174 assembling method, innovative structures may be designed with applications to material science,
175 architecture and engineering mechanics (Reis et al. 2015).

176 Working with *objects* such as grains is different from dealing with *laws* governing a continuum
177 in that the grains materialize the degrees of freedom of a packing. It is maybe this essence that
178 makes granular materials so accessible and attractive to many people. Deriving coarse-grained laws
179 arising from the collective behavior of grains is a fundamental research goal. This has been and will
180 be the goal of soil mechanics, which has a long background of engineering practice and deals with
181 granular materials on an everyday basis. The increasing interest in the grain-scale behavior and
182 micro-mechanical approach is not just a luxury. It reflects a real need for enhanced understanding
183 and predictive modeling of soils and powders (Mitchell and Soga 2005). In this endeavor, continuum
184 mechanics provides the framework for a rational analysis but the shift towards multi-scale modeling
185 is unavoidable. The query is how much of the rich information obtained at the micro-scale is relevant
186 to the macro-behavior.

187 In the following, the authors discuss some major milestones in each of the aspects briefly men-
188 tioned above. In practice, these aspects are developed by different communities and their relation-
189 ships are not always well understood. But it is useful to mention here, even very briefly, relevant
190 contributions for a broad understanding of the field. The first section reviews classical continuum
191 modeling as elaborated, essentially in the soil mechanics community, before roughly 1990. Next, the
192 particle-scale behavior is considered in terms of granular texture, force transmission and particle
193 displacements, followed by a number of bottom-up developments based on particle-level investiga-
194 tions, which benefited, in the three last decades, from a renewed interest in the condensed matter
195 physics laboratories, and from micromechanical approaches. Finally, more recent developments in
196 macroscopic modeling are reviewed. The last section will describe some of the new frontiers and
197 open issues for future research.

198 **CONTINUUM MODELS**

199 Granular materials can be found in gas-like, liquid-like and solid-like states, but, unlike molec-
200 ular systems, they are governed by dissipative interactions and steric constraints that make their
201 behavior depend on both pressure level and porosity. Furthermore, as in colloids and foams, their
202 plastic deformations are controlled by substantial evolution of particle arrangements. In this sec-
203 tion, the foundations of the continuum models of granular behavior are briefly discussed with
204 pressure, void ratio and anisotropy as basic variables.

Critical State Theory (CST)

Granular materials are characterized by both material variability (grain shapes and size distributions, grain surface properties . . .) and microstructural variability (organization of grains and their contacts). The incremental stress-strain response of a granular material depends on minute details of its microstructural state, encoding the past deformations and stresses experienced by the material, as shown in Fig. 1. Under complex loading, the microstructure evolves but the memory of the initial state persists and determines the mechanical response. For this reason, the possibility of a unique constitutive framework for the plastic behavior of granular materials with measurable internal variables remained out of reach for a long time. However, a host of mechanical tests on soils in the first half of the 20th century gradually established the fact that a sheared soil tends to a well-defined state in which the memory of the initial state is fully lost.

In this *critical state* (CS), as put by Casagrande and formulated by Roscoe et al. in 1958, the behavior of granular materials can be described by relationships among shear strength, mean effective stress p and void ratio e (or equivalently packing fraction $\rho = 1/(1+e)$) (Casagrande 1936; Roscoe et al. 1958). Using $p = tr(\sigma_{ij})/3$ and $q = (3s_{ij}s_{ij}/2)^{1/2}$, where σ_{ij} is the effective stress tensor carried by the granular backbone and $s_{ij} = \sigma_{ij} - p\delta_{ij}$, the CS is generally described by two relationships (Schofield and Wroth 1968; Wood 1990):

$$\eta = \frac{q}{p} = M(\theta_L) \quad (1)$$

$$e = f(p/p_i) \quad (2)$$

where $f(p/p_i)$ is a function of the effective mean stress p and characteristic stresses p_i of the material such as the crushing strength or the cohesive strength, and M characterizes the frictional behavior depending on φ and intermediate stress σ_2 via Lode angle θ_L . An important observation is that the CS may well be localized inside a sub-volume such as a shear band (Coumoulos 1967). The Critical State Theory (CST) is based on the assumption of homogeneity and isotropy of the material. Objective strains can only be measured in a volume where uniform deformation occurs.

The identification of CS makes it also possible to characterize different states of a granular sample by *state variables* based on the “distance” from the CS (Been and Jefferies 1985; Jefferies 1993). This is, for example, the case for void ratio e , whose evolution largely depends on its

233 distance $\Psi = e - e_c$, as a *state parameter*, from the CS line $e_c(p)$, dilatant if below the CS line and
 234 contractant if above the CS line. The function f in (2) may also depend on the lowest and largest
 235 void ratios, e_{min} and e_{max} , accessible to a granular material (depending on its grain properties).
 236 For example, the following fitting form provides a simple function that works reasonably well for
 237 sands (Verdugo and Ishihara 1996):

$$238 \quad e = e_{max} - \frac{e_{max} - e_{min}}{\log(p_i/p)} \quad (3)$$

239 As will be seen below, the state parameter Ψ , with its variants, plays a central role in most
 240 constitutive models developed for sand. ‘

241 **Stress-dilatancy relation**

242 Besides critical states, which reflect self-sustaining microstructures of a granular material under
 243 monotonic shearing, energetic considerations were used to derive the first constitutive models of
 244 sands and soils. The fact that both stress ratio and void ratio vary with shear strain led Taylor
 245 to consider the work done by shear and dilation and formulate a *stress-dilatancy* relation in 1948
 246 (Taylor 1948). Let $\dot{\epsilon}_p$ and $\dot{\epsilon}_q$ be the volumetric and shear deformation rates in a planar shear flow.
 247 The total rate of supplied work is $\dot{W} = q\dot{\epsilon}_q + p\dot{\epsilon}_p$. Hence,

$$248 \quad \eta = \frac{q}{p} = -\frac{\dot{\epsilon}_p}{\dot{\epsilon}_q} + \frac{\dot{W}}{p\dot{\epsilon}_q} \quad (4)$$

249 For a constant value of $p\dot{\epsilon}_q$ (shear rate and mean stress being imposed) and assuming that \dot{W}
 250 is nearly constant, equation (4) suggests a linear relation between η and dilatancy defined by
 251 $D = -\sin \psi \equiv \dot{\epsilon}_p/\dot{\epsilon}_q$. The dilatancy D vanishes in the CS and, according to (4), $\eta = M = \dot{W}/p\dot{\epsilon}_q$
 252 in the critical state so that

$$253 \quad \eta = D + M \quad (5)$$

254 The above relation is in good agreement with experiments and simulations only in a limited
 255 range of stresses. Alternative versions of this relation did not alter the fundamental conclusion that
 256 dilatancy plays a major role in stress-strain behavior of granular materials (Newland and Allely
 257 1957; Rowe 1962; Nova 1982; Bolton 1986). In particular, it controls the shear peak in dense sand
 258 and compaction for loose sand. To account for experimental observations, it was modified by Nova

259 by introducing a new parameter N such that $\eta = (N - 1)D + M_\theta$ with the material-dependent
 260 parameter N (Nova 1982). The value of the latter is observed to be $\simeq 0.2$ (Jefferies and Been 2006).

261 However, a more fundamental criticism was introduced by Li and Dafalias (Li and Dafalias
 262 2000). By recalling the basic observation that the same value of η may give rise to either contractive
 263 or dilatant behavior depending on the current void ratio and/or mean pressure, they remarked that
 264 dilatancy can not be a unique function of the stress ratio η (unless little change occurs in the internal
 265 state) but it should depend on the current state of the material. They showed that major effects
 266 of the current void ratio and effective stress can indeed be captured by making depend D on the
 267 state parameter $\Psi = e - e_c$ in such a way that D vanishes for $\Psi = 0$ and $\eta = M$. This requirement
 268 is satisfied by the function

$$269 \quad D = D_0 \left(e^{m\Psi} - \frac{\eta}{M} \right), \quad (6)$$

270 where D_0 and m are material parameters. This function suggests that the dilatancy D depends on
 271 the difference of the current stress ratio η from a reference stress ratio $Me^{m\Psi}$, as in Rowe's stress-
 272 dilatancy theory but with the difference that this reference stress ratio varies with Ψ instead of
 273 being fixed. A similar concept was actually used by Manzari and Dafalias for constitutive modeling
 274 (Manzari and Dafalias 1997).

275 **Constitutive models of granular plasticity**

276 It is important to emphasize that the CST is not a constitutive model but a theoretical expres-
 277 sion of robust observational facts. The granular behavior can be described by various elasto-plastic
 278 constitutive models of increasing complexity incorporating the CS as a reference state (Manzari
 279 and Dafalias 1997; Radjai and Roux 2004; Li et al. 2012; Gao et al. 2014). Cam-Clay model was the
 280 first consistent constitutive model based on the CST and Taylor's stress-dilatancy relation, together
 281 with the assumptions of associated plasticity and isotropy (Roscoe and Schofield 1963; Schofield
 282 and Wroth 1968). In this framework, the stress-dilatancy relation is used to derive a yield surface
 283 in which the pre-consolidation pressure plays the role of history parameter. The predictions of this
 284 model and its modified version, in both drained and undrained triaxial tests reproduce correctly
 285 many observed features of clay behavior under triaxial conditions. The gradual plastification of the
 286 clay before stress peak is accounted for by introducing a sub-loading surface evolving isotropically
 287 with the state parameter (Hashiguchi 1979; Hashiguchi and Chen 1998).

288 Nor-Sand is a model similar to Cam-Clay based on the CST but specialized to sand (Jefferies
 289 1993). The yield surface is derived from Nova's stress-dilatancy relation (Nova 1982), and the
 290 pre-consolidation pressure is replaced by the critical state pressure. Nova's stress-dilatancy relation
 291 leads to the following yield function:

$$292 \quad F = \eta - M_\theta \left\{ 1 + (N - 1) \left(\frac{p}{p_i} \right)^{N/(N-1)} \right\} \quad (7)$$

293 where p_i is a pressure parameter replacing p_c and representing the critical state pressure. To account
 294 for plastic hardening, it is further assumed that the stress state lies on a sub-loading surface similar
 295 to the above yield surface with varying value of p_i until a limit value p_i^{max} is reached. In other
 296 words, p_i scales the size of the yield surface. The surface evolves as a function of the state parameter
 297 Ψ . The pressure p_i^{max} is a reference parameter from which the evolution of the p_i can be simply
 298 modeled by a linear law: $\partial p_i / \partial \varepsilon_p = H(p_i^{max} - p_i)$, where H is the hardening modulus.

299 The isotropic nature of the plastic model used in Nor-Sand and similar models, makes them
 300 inadequate for modeling cyclic behavior. Volumetric hardening models are adequate for clays, but
 301 for granular materials the shear hardening is an essential ingredient. For this reason, and also due
 302 to practical calibration problems, later developments in this framework focused mainly on a more
 303 general plastic framework with kinematic hardening (Mroz et al. 1978; Manzari and Dafalias 1997).

304 These concepts are more particularly incorporated in SANISAND, the name for a class of
 305 Simple ANIsotropic SAND constitutive models extended from the original two-surface plasticity
 306 model developed by Manzari and Dafalias (Manzari and Dafalias 1997; Dafalias and Manzari 2004;
 307 Taiebat and Dafalias 2008). This model is based on the CST and bounding surface plasticity, which
 308 represents the memory of the material. It uses a narrow open cone-type yield surface obeying
 309 rotational (kinematic) and isotropic (volumetric) hardening. The rotational hardening is assumed
 310 to reflect the evolution of structural anisotropy. The plastic strain rate is composed of two parts
 311 resulting, respectively, from the change of stress ratio (dilatancy) and loading under constant
 312 stress ratio. The isotropic hardening depends on the volumetric component of the latter. This
 313 model is non-associated and the state parameter Ψ is used to define the peak and dilatancy stress
 314 ratios. When calibrated by experiments, it is able to correctly describe the behavior of sand under
 315 general conditions, both monotonic and cyclic. It should be noted that the most recent constitutive

316 models account for the anisotropy and its evolution by extending the concept of the critical state
317 and introducing state-dependent stress-dilatancy relations (Li et al. 2012; Gao et al. 2014). Such
318 models account naturally for the non-associated feature of flow rule and non-coaxiality between
319 strains and stresses (see section 5).

320 The above models assume the concept of simple materials (Noll 1955), which implies that the
321 material behavior can be fully characterized under homogeneous strains. Shear banding, however,
322 seems to counter this assumption. One of the early constitutive models fully based on slip planes
323 was the dilatant double shearing model of Mehrabadi and Cowin (Mehrabadi and Cowin 1978). In
324 this model, it is assumed that the deformation of a granular material is composed of two dilatant
325 shear deformations along the stress characteristics, which are interpreted as slip lines. This model
326 in its later developments was enriched by incorporating elastic deformation, plastic work hardening
327 and, more recently, the fabric tensor (Nemat-Nasser et al. 1981; Zhu et al. 2006). The shear rates
328 along the two slip systems are related to the density of contacts along them. While several internal
329 variables introduced in the model are phenomenological, the model can describe monotonic and
330 cyclic responses of granular materials, the evolution of void ratio and the evolution of fabric tensor
331 with the stress tensor (see section 3).

332 It is useful to briefly mention also here the framework of hypoplasticity, which was developed
333 with the strong idea of finding the most general and objective expression of the stress rate $\dot{\sigma}$ as a
334 function of the current stress state σ and velocity gradient tensor D (Kolymbas 1991; Kolymbas
335 et al. 1995; E. 1996; Gudehus 1996; Lanier et al. 2004). The application of representation theorems
336 of isotropic functions leads to a generically nonlinear dependence of the material behavior on the
337 direction of strain rate. The incremental nonlinearity being intrinsic to the evolution equation,
338 there is no need to explicitly distinguish between loading and unloading paths. This framework
339 postulates no yield function and flow rule, and the usual partition of the strain-rate tensor into
340 elastic and plastic parts disappears. However, those concepts can be obtained as predictions of the
341 model for different forms and values of model parameters (Wu and Niemunis 1996).

342 Advanced hypoplastic models account for void ratio as scalar state variable and pressure level,
343 as well as the critical state (Huang et al. 2008; Masin 2012; Fuentes et al. 2012). The tensorial fabric
344 state can also be incorporated in the model at the price of extending the framework and number of
345 material parameters (Wu 1998). The latest developments tend to show that almost all elasto-plastic

346 models can be equally formulated in the hypoplastic framework (Huang et al. 2006). A unification
347 was actually achieved by Einav, who considered the class of hypoplastic models that are compatible
348 with thermodynamics and showed that elasto-plasticity is a singular limit of hypoplasticity (Einav
349 2012).

350 Another general framework applied to granular materials is that of micropolar theories, which,
351 by introducing a length scale into their continuum description, offer the possibility of accounting for
352 size effects, e.g. in shear banding. This length may be interpreted as the scale below which particle
353 rotations can significantly differ from those deduced from the rotational of the displacement field.
354 At a larger scale the difference vanishes and thus, upon coarse-graining, the standard theory is
355 recovered (Tejchman and Wu 1993). These models attribute micro-rotations and couple stresses to
356 material points, extending thus the number of constitutive relations for elastic and plastic behavior.
357 In association with hypoplasticity, they can lead to realistic results in large deformations with shear
358 banding (Grammenoudis and Tsakmakis 2005).

359 **Elastic behavior**

360 An elastic or quasi-elastic response is observed in granular materials when small stress incre-
361 ments are added to a pre-stressed equilibrium configuration by static or dynamic (resonance, sound
362 propagation) experiments. The linear response to such increments is then, as a good approxima-
363 tion, reversible, and associated to some quadratic elastic energy, the initial prestressed configuration
364 defining the reference state, which is at the origin of elastic displacements and strains. An elastic
365 model applies, for sands stabilized under confining stresses between 10 kPa and a few MPa, to
366 strain intervals not exceeding some limit of order 10^{-6} or 10^{-5} (Hicher 1996; Shibuya et al. 1992;
367 Kuwano and Jardine 2002; Geoffroy et al. 2003). For larger strains, the dissipation is no longer
368 negligible in stress-strain cycles.

369 The accuracy of strain measurements in soil mechanics has made significant progress over the
370 last decades, and measurements in the very small strain, quasi-elastic regime, about differently
371 prestressed states are now feasible. Static measurements of elastic moduli agree with dynamic
372 measurements deduced from resonance wave frequencies or propagating wave speeds (Thomann
373 and Hryciw 1990; Shibuya et al. 1992; Geoffroy et al. 2003). The elastic moduli should not be
374 confused with the slopes of stress-strain curves on the strain scale (say, of the order of 1%) corre-

375 sponding to the mobilization of internal friction. Those slopes are considerably smaller than true
 376 elastic moduli, by more than an order of magnitude, and do not correspond to an elastic response.
 377 Simplified elastic-plastic models (Vermeer 1998) used in engineering applications, in which the ma-
 378 terial is linear elastic until the Mohr-Coulomb criterion for plasticity is reached, corresponding to
 379 full internal friction mobilization, should not be misinterpreted: the elastic part of the material
 380 behavior in such models is essentially a computationally motivated simplifying assumption.

381 **PARTICLE-SCALE BEHAVIOR**

382 Granular materials are disordered at the micro-scale with strong fluctuations of particle envi-
 383 ronments from one particle to another. Within the rigid-particle approximation, the local behavior
 384 can be described by vectorial quantities (branch vectors, contact forces), which underly macroscopic
 385 tensorial variables (stress, strain, fabric). In this section, the main features of granular texture,
 386 force transmission and particle displacements are discussed.

387 **Granular texture**

388 In a fundamental approach, the state parameters are of geometrical nature. Such descriptors
 389 of the texture are generally known as *fabric* parameters. The level of description depends on the
 390 choice of these parameters, which should naturally comply with both the accuracy and tractability
 391 of the formulation and which can be scalar or tensorial parameters or functions. Two constraints
 392 make the plastic behavior of granular materials depend on nontrivial aspects of the microstructure:
 393 1) the steric hindrances among neighboring particles, which constrain the accessible geometrical
 394 states, and 2) the condition of mechanical equilibrium, which controls to some extent the range of
 395 admissible particle configurations (Roux and Radjai 2001; Troadec et al. 2002; Radjai 2009).

396 Figure 2(a) displays a representation of the contact geometry between two neighboring particles.
 397 The relevant geometrical variables are the *contact vector* \vec{r} joining the particle center to the contact
 398 point, the *branch vector* $\vec{\ell}$ joining the centers of two contacting particles and the contact orientation
 399 vector (contact normal) \vec{n}' defined as the unit vector normal to the particle boundary at the contact
 400 zone α . The reaction forces \vec{f} and $-\vec{f}$ acting on the two particles at their contact zone have a unique
 401 application point that may be considered as their contact point. The local frame is composed of
 402 the radial unit vector \vec{n} and one orthogonal unit vector \vec{t} in an ortho-radial plane (orthogonal to
 403 the contact vector). In 2D, the local frame is uniquely defined by a single tangent unit vector \vec{t} .

404 One needs a statistical description due to granular disorder, with the basic feature that the
 405 local vectors vary discontinuously from one contact to another. The local environments fluctuate
 406 in space both in the number k of the contacts of each particle (topological disorder) and in their
 407 angular positions \vec{r}^α (metric disorder). For the formulation of the local constraints only the first
 408 contact neighbors of a particle are sufficient. Two functions are required to describe this *first shell*
 409 environment (Roux and Radjai 2001; Troadec et al. 2002):

- 410 1. $P_c(k)$: *Connectivity function* defined as the proportion of particles with exactly k contacts
 411 (first shells with k members).
- 412 2. $P_{kkrf}(\vec{r}^1, \dots, \vec{r}^k, \vec{f}^1, \dots, \vec{f}^k)$: *Multicontact probability density function* of k contact forces \vec{f}^α
 413 and k angular positions \vec{r}^α for a shell of k particles.

414 The average connectivity of the contact network is the coordination number $z = \sum_{k=1}^{\infty} kP_c(k)$.
 415 Integration of P_{kkrf} over all angular positions yields the multicontact force pdf's $P_{kkf}(\vec{f}^1, \dots, \vec{f}^k) =$
 416 $\int_{\mathcal{A}_{kr}} P_{kkrf} d\{\vec{r}^\alpha\}$, where \mathcal{A}_{kr} is the accessible domain of angular positions. In the same way, the
 417 multicontact pdf of angular positions is $P_{kk}(\vec{r}^1, \dots, \vec{r}^k) = \int_{\mathcal{A}_{kf}} P_{kkrf} d\{\vec{f}^\alpha\}$, where \mathcal{A}_{kf} is the
 418 integration domain. In the particle shells, the steric constraints manifest themselves as *angular*
 419 *exclusions*. Two particles belonging to a shell cannot approach one another below a minimum
 420 angular interval $\delta\theta_{min}$; see Fig. 2(b). In other words, the multicontact probability density P_{kk}
 421 vanishes if the angular exclusions are violated.

422 These multicontact probability density functions are too rich to be accessed experimentally or
 423 tackled theoretically. The information that they contain can be reduced in three steps. In the first
 424 step, one extracts the 1-contact distributions for the shells of k contacts by integration over all
 425 contacts except one. In the second step, the 1-contact distributions are averaged over the shells by
 426 weighting them by P_c . The third step consists in extracting the angular behavior. In particular,
 427 the probability density function $P(\vec{n})$ of contact normals is often used to represent the structural
 428 anisotropy. Its second moment $\mathbf{F} = \langle \vec{n} \otimes \vec{n} \rangle \equiv \int_{\Omega} \vec{n} \otimes \vec{n} P(\vec{n}) d\vec{n} / 2\pi$, where Ω denotes the angular
 429 domain, defines the *fabric tensor* \mathbf{F} with $\text{tr}(\mathbf{F}) = 1$. The lowest-order anisotropies of the contact
 430 network are given by $a_c^{ij} = 2(F_i - F_j)$, where F_1 , F_2 and F_3 are the principal values of \mathbf{F} (Oda et al.
 431 1980; Satake 1982; Rothenburg and Bathurst 1989; Cambou 1993; Radjai et al. 1998; Kuhn 1999;
 432 Ouadfel and Rothenburg 2001). Higher-order moments and anisotropies can also be extracted from

433 $P(\vec{n})$.

434 Obviously, the fabric anisotropy can equivalently be defined from other characteristic orien-
435 tations such as those of branch vectors (joining particles centers) or voids, which generally have
436 elongated shapes (Satake 1982; Kuhn 1999). The choice should naturally be guided by the mod-
437 eling approach and the variables of interest. The yield function is more closely related to contact
438 anisotropy or branch-vector anisotropy since the condition of force balance is enforced at the level of
439 each particle with forces exerted by neighboring particles whereas the flow rule reflects the evolution
440 of void volumes for which the compatibility condition of particle displacements can be formulated,
441 and hence the void anisotropy and valence number (average number of particles in a loop of par-
442 ticles) seem to be essential; see Fig. 2(c). The connection between these two anisotropies is an
443 important ingredient for relating local strains and stresses in a micromechanical approach (Roux
444 and Radjai 2001). A related aspect is the scale at which the fabric is defined. Particle-scale fabrics
445 are fluctuating variables both in space and in time. They are well-defined only at a mesoscopic
446 scale. In this sense, the averaged fabric tensors are macroscopic objects and their use in a macro-
447 scopic model assumes that the Representative Volume Element (RVE) exists not only for stresses
448 and strains but also for the fabric tensors. In contrast, a micromechanical approach should be based
449 on particle-scale fabric variables, which incorporate the constraints of force balance and kinematic
450 compatibility (Trodec et al. 2002).

451 **Stress transmission**

452 The distribution of contact forces in model granular materials has been extensively studied
453 initially by experiments and later amplified by Discrete Element Method (DEM) simulations. Geo-
454 metrical exclusions and disorder in granular materials lead to a highly inhomogeneous distribution
455 of forces (Dantu 1957; Drescher and de Josselin de Jong 1972; Liu et al. 1995; Radjai et al. 1996;
456 Thornton 1997; Mueth et al. 1998; Radjai et al. 1999; Majmudar and Behringer 2005; Miller et al.
457 1996). Filamentary patterns of stresses observed on photoelastic images are induced by strong
458 contact forces and are known as *force chains*. The forces were more accurately measured by using
459 carbon paper to record normal force prints at the boundaries of a bead packing (Mueth et al. 1998).
460 They were found to have a nearly uniform probability density function (pdf) in the range of weak
461 forces followed by an exponential falloff of strong forces. Similar force distributions were found by

462 means of numerical simulations (Radjai et al. 1996; Thornton 1997; Radjai and Wolf 1998; Radjai
463 et al. 1999; Antony 2001).

464 All further investigations of force distributions have shown that the exponential distribution
465 of strong forces is a robust feature of granular media. In contrast, the weak forces appear to be
466 sensitive to the packing state resulting from the deformation history (Antony 2001; O’Hern et al.
467 2001; Snoeijer et al. 2004). In an isotropic packing state, the distribution shows a relatively small
468 peak below the mean force, and the probability density of small forces does not fall to zero (Metzger
469 2004a; Metzger 2004b). The peak disappears in a sheared packing and the distribution of weak
470 forces turns to a nearly decreasing power law (Radjai et al. 1999; Antony 2001; Azéma and Radjai
471 2014). Fig. 3(a) shows a map of contact forces in a strongly polydisperse packing. This is what
472 generally is observed in frictional packings composed of aspherical grains or broad size distributions
473 (Voivret et al. 2009; Azéma et al. 2007; Azéma et al. 2009; Saint-Cyr et al. 2011; Azema et al.
474 2013; Nguyen et al. 2014). Increasing the confining stress of elastic grains leads to considerable
475 deformation of the grains and increase of the coordination number beyond its rigid limit value,
476 while the force distribution tends to assume a narrower nearly Gaussian shape (Makse et al. 2000;
477 Agnolin and Roux 2007b).

478 The q -model was the first statistical model of force distributions (Liu et al. 1995; Coppersmith
479 et al. 1996). The forces are assumed to be scalar quantities that “propagate” from site to site
480 (particles) along the links (contacts) of a regular network. The total incoming force from the
481 particles of a layer to each site is redistributed to the particles of the next layer according to a
482 random process. This model predicts that the force pdf converges to a purely exponential function
483 $P(f) = \beta e^{-\beta f}$ with the exponent β depending on the number of supporting contacts per grain. A
484 statistical approach developed by Metzger et al. provides a correct estimate of the force pdf by
485 analyzing the local constraints and accounting for the density of states in a first-shell approximation
486 (one grain with its contact neighbors) (Metzger 2004b). Another simple analytical model based
487 on the assumption that a force of a given value can only be generated from the population of
488 higher forces but requires weaker forces for its equilibrium, leads to an expression with a single free
489 parameter that fits well the force distributions (Radjai 2015).

490 Detailed analysis of sheared dry granular materials provides evidence for the *bimodal* organiza-
491 tion of the force network in well-defined “weak” and “strong” networks, with the strong network

492 contributing almost exclusively to the shear strength, and weak forces acting mainly to prop strong
493 force chains (Radjai et al. 1998; Radjai et al. 1999). The supportive effect of weak forces is re-
494 flected in the anisotropy of weak contacts with their privileged direction that is perpendicular to
495 that of strong contacts. In the case of polygonal grains in 2D, this supportive action appears in
496 the anisotropy of the weak forces rather than weak contacts (Azéma et al. 2007).

497 In the absence of stress gradients (macroscopically homogeneous shear), the forces below the
498 mean are in the weak network, which contains nearly 60% of contacts, which sustain 25 % of
499 the average stress. Nearly all sliding contacts during shear belong to this network, i.e. plastic
500 dissipation occurs almost fully in this network. But since the partial shear stress through this
501 network is nearly zero, from a mechanical viewpoint it is a liquid-like phase whereas the strong
502 network behaves as a solid skeleton for the medium. This bimodal feature suggests that granular
503 materials can be modeled as two-phase media with two stress tensors (Zhu et al. 2006).

504 **Granular kinematics**

505 Kinematic fields (particle translations and rotations) at the particle scale in sheared granular
506 materials have complex patterns that have been much less investigated than contact force distri-
507 butions in exception to shear localization, which has for a long time been associated with failure
508 at peak stress ratio. DEM simulations show that even at early stages of shear deformation, well-
509 organized *micro-bands* of intense shearing occur despite overall homogeneous boundary conditions
510 (Kuhn 1999; Lesniewska and Wood 2009). These micro-bands evolve rapidly in space and time,
511 and the shear bands at larger strains seem to arise as a result of their coalescence.

512 Grain rotations and rolling contacts play a crucial role in the local kinematics of granular
513 materials. Shear zones are generally marked by intense particle rotations (Oda et al. 1982; Kuhn
514 and Bagi 2004). Since rolling contacts dissipate much less energy than sliding contacts, grain
515 motions in quasi-static shear occur mostly by rolling. Sliding contacts are actually a consequence
516 of the frustration of particle rotations in the sense that all contacts within a loop of contiguous
517 particles cannot be simultaneously in rolling state. The basic structure of a loop of three grains
518 illustrates well this property (Tordesillas 2007). For this reason, it has been argued that such
519 mesoscopic structures evolve and their statistics is correlated with plastic hardening and softening
520 of granular materials. In general, long-range correlations, as those reflected in the structure of force

521 chains, indicate that single-contact models cannot fully capture the local behavior. A correlation
522 length of the order of 10 grain diameters is observed in forces (Staron et al. 2005). As an internal
523 length scale, it can be related to the thickness of shear bands.

524 Another important feature of particle velocity fields is that, as a result of steric exclusions, the
525 particle velocities $\{\vec{r}^i\}$ have a non-affine fluctuating component $\{\vec{s}^i\}$ of zero mean with respect to
526 the background shear flow, as displayed in Fig. 3(b) (Radjai and Roux 2002; Peters and Walizer
527 2013; Combe et al. 2015). These fluctuating velocities have a scaling behavior which is very similar
528 to those of fluid turbulence and were therefore coined by “granulence” by Radjai and Roux (Radjai
529 and Roux 2002). In particular, the velocity probability density functions undergo a transition
530 from stretched exponential to Gaussian as the time resolution is increased, and the spatial power
531 spectrum of the velocity field obeys a power law, reflecting long-range correlations and the self-
532 affine nature of the fluctuations. These observations contradict somehow the conventional approach
533 which disregards kinematic fluctuations in macroscopic modeling of plastic flow in granular media.
534 The long-range correlations of velocity fluctuations may be at the origin of the observed dependence
535 of shear stress on the higher-order gradients of shear strain, implying that granular materials are
536 not “simple” materials in the sense of Noll (Kuhn 2005; Noll 1958).

537 A key aspect of granular kinematics is its discontinuous evolution. The contacts between par-
538 ticles have a short lifetime and new contacts are constantly formed as the particles move. The
539 overall picture is that more contacts are gained along the directions of contraction and lost along
540 the directions of extension (Rothenburg and Bathurst 1989). A detailed balance equation can be
541 written for the evolution of contacts along different directions. Only in the critical state the rates
542 of gain and loss are equal (Radjai et al. 2004; Radjai et al. 2012). However, this is only an average
543 picture and the effects of the chaotic fluctuating velocity field are not yet well understood (Pouya
544 and Wan 2016). They may well behave as a noise or control the fabric evolution under complex
545 loading conditions. When the direction of shear is reversed, for example, there is a clear asym-
546 metry between the gain and loss processes, which leads to a decrease of the coordination number
547 whereas the void ratio decreases at the same time (Radjai and Roux 2004). Such effects control
548 the nonlinear behavior of granular materials under complex loading paths.

549 **BOTTOM-UP APPROACH**

550 Beyond experimental validation, macroscopic models of granular behavior must provide a clear
551 physical basis for their internal variables (or state parameters) at the grain scale. Considerations on
552 grain-level mechanics and statistics of contact networks and their rearrangements, on the one hand,
553 and ideas from condensed-matter physics and soft matter rheology, on the other hand, triggered
554 or inspired different methods for bottom-up (micro-macro) modeling of granular materials that are
555 discussed in this section.

556 **Numerical and multiscale modeling**

557 The bottom-up modeling refers to an approach fully or partially based on the particle interac-
558 tions and granular texture. This implies upscaling through at least five scales: contact, particle,
559 assembly, representative volume element (RVE) and structure, as schematized in Fig. 4. The up-
560 scaling from the contact scale is mediated by particles (where equilibrium conditions are defined),
561 and their assembly in mesoscopic microstructures (where compatibility conditions are defined).

562 Besides extraordinary progress made in measurement techniques, computerized testing and
563 imaging devices such as micro-tomography, the DEM (Discrete Element Method) allows accurate
564 simulations of stiff particles for complex loading and significant cumulative strains. This has made
565 it possible to characterize granular texture, force transmission and particle motions, and to address
566 long-lasting issues such as the role of fluctuations, partial stresses carried by a specific class of
567 contacts or particles . . . , which are clearly much more complex than naive pictures of local behavior
568 used sometimes in earlier developments. Such details are, however, not straightforward to fit
569 into continuum modeling approaches. Hence, the issue is to identify the lowest-order geometrical
570 parameters that should be incorporated in a macroscopic model and understand the extent that
571 mechanical behavior depends on higher-order parameters. This approach is not straightforward
572 and has many drawbacks compared to advanced constitutive models, but will lead in the long run
573 to predictive models.

574 However, the DEM is not yet computationally efficient for solving boundary-value problems at
575 large scales with large number of particles. For this reason, the DEM can be used as a means
576 to access the meso-scale (scale of an assembly of grains) information, which can then be upscaled
577 to the continuum level using the Finite Element Method (FEM) or averaging techniques (Kaneko

578 et al. 2003; Andrade and Tu 2009; Nitka et al. 2011; Andrade et al. 2011; Guo and Zhao 2016;
579 Liu et al. 2016). Most of the recent work in the physics community addresses the first stage,
580 i.e. the description of meso-scale structures from the grain-scale, whereas many micromechanical
581 models are concerned with the second stage in which the meso-scale is represented as a continuous
582 distribution of contact planes.

583 The multiscale approach is often mentioned as an alternative to purely numerical DEM or
584 micromechanical approaches. The FEM is employed to solve a boundary value problem while
585 using the DEM to derive the required nonlinear material responses at each FEM Gauss integration
586 point. Hence, this approach requires no constitutive model as in the conventional FEM simulations.
587 The accuracy of the model depends on the number of Gauss points (FEM discretization) and
588 the number of particles associated with each point (DEM discretization). This approach should
589 therefore be considered as a hierarchical coupling approach and an integrated tool for solving
590 boundary-value problems. But it should not elude a theoretical micromechanical approach with
591 the goal of basing macroscopic models on internal variables pertaining to the granular texture for a
592 better understanding the origins of the complex phenomenology of granular materials.

593 **Stress and strain tensors**

594 The discrete nature of granular materials makes them different from composites or other inho-
595 mogeneous materials usually considered in micromechanics. In particular, the macroscopic tenso-
596 rial variables such as stress and strain must be constructed from statistical averages of vectorial
597 variables such as contact forces and relative displacements of grains over representative volume ele-
598 ments (RVE). As pointed out by He, the definition of macroscopic stress and strain tensors should
599 be based on the boundary data of a RVE since they should satisfy the equilibrium and compati-
600 bility equations, respectively (He 2014). For granular materials, the expression of the stress tensor
601 as a function of contact forces and branch vectors is classical since equilibrium conditions are well
602 defined (Love 1929) whereas compatibility equations are less well formulated.

603 The approach recently introduced by He consists in considering grain centers and taking the
604 domain generated and partitioned by the Delaunay tessellation as the domain of a representative
605 volume element filled with a continuum medium (He 2014). Following a similar work by Kruyt
606 and Rothenburg in 2D (Kruyt and Rothenburg 1996), the 3D compatibility equations for the

607 grain center displacements is thus established and an explicite micromechanical expression for the
 608 macroscopic strain rate is derived. The expressions of stress and strain rate tensors are

$$609 \quad \sigma_{ij} = n_c \langle f_i \ell_j \rangle_c \quad (8)$$

$$610 \quad \dot{\varepsilon}_{ij} = n_p \langle \delta \dot{u}_i a_j + \delta \dot{u}_j a_i \rangle_p / 2V \quad (9)$$

611 where n_c is the number density of contacts, n_p is the number density of neighboring grain pairs
 612 (pairs of grains in contact or separated by a small gap), ℓ_j is the j -component of the branch vector
 613 joining grain centers, f_i is the i -component of contact force, V is the total volume, $\delta \dot{u}_i$ is the
 614 i -component of the relative velocity between two neighboring grains, and a_j is the j -component
 615 of the area vector perpendicular to the Delaunay plane separating the the two grains. The first
 616 averaging runs over all contacts c whereas the second one runs over all adjacent pairs of grains.

617 **Granular elasticity**

618 The elasticity of a granular packing is a direct consequence of the elasticity of particles, as ex-
 619 pressed in contact laws (Johnson 1985). Elastic moduli of granular packings are primarily sensitive
 620 to the stress level, via the average contact stiffness, which is proportional to $P^{1/3}(z\phi)^{-1/3}$ under
 621 pressure P , where ϕ is the solid fraction and z is coordination number, if contacts are Hertzian
 622 (factor $z\Phi$, expressing the contact density, appears here because the average contact force scales
 623 as $P/(z\Phi)$ (Agnolin and Roux 2007a)). Assuming contacts through angular asperities (Johnson
 624 1985), local stiffnesses should rather scale as $P^{1/2}(z\phi)^{-1/2}$. Such power law stress dependences are
 625 experimentally or numerically observed, with, most often, an exponent slightly larger than 1/3 for
 626 spherical particles (Kuwano and Jardine 2002; Agnolin and Roux 2007c), or than 1/2 for angular
 627 sand grains (Hicher 1996). This difference between predicted and measured exponent values might
 628 partly be attributed to the change of contact numbers under varying stresses (Goddard 1990b),
 629 although increases of coordination numbers under growing stresses is mostly influential (Makse
 630 et al. 1999; Agnolin and Roux 2007c) under rather large confining stress levels (in the MPa range).

631 Recent numerical studies show that the departure from theoretical exponents, under lower pres-
 632 sure, is most often due to the singular properties of poorly connected networks (Wyart 2006; Somfai
 633 et al. 2005), in which the small degree of force indeterminacy entails (Wyart et al. 2005) a large
 634 excess of “soft modes”, associated to anomalously low eigenvalues of the contact network stiffness

635 matrix, in comparison to those of a homogeneous elastic continuum. In the limit of vanishing
636 force indeterminacy, which is indeed approached for small stresses with frictionless objects (Roux
637 2000; Silbert et al. 2002), the moduli tend to scale with the degree of force indeterminacy per unit
638 volume (Wyart 2006; Agnolin and Roux 2007c; Somfai et al. 2007), whence a proportionality to
639 the difference between the coordination number of the force-carrying network and its minimum
640 (isostatic) value: to $z - 6$ for frictionless spheres, or to $z - 4$ for frictional ones. The resulting
641 anomalously low moduli increase faster with pressure, as they are sensitive to small increases of co-
642 ordination numbers. This is apparent in Fig. 5, showing an increase of shear moduli with pressure,
643 for poorly coordinated sphere packings, with an exponent notably larger than the theoretical value
644 $1/3$. Such effects, in isotropic systems, do not influence the bulk modulus, for which simple predic-
645 tions based on the Voigt assumption of affine elastic displacement fields provide reasonable approx-
646 imations (Somfai et al. 2007; Agnolin and Roux 2007c). For anisotropic stress states (Peyneau and
647 Roux 2008b), the non-singular modulus is the one associated with stress increments proportional
648 to the pre-existing stress values.

649 Figure 5 also illustrates the greater sensitivity of moduli to coordination number z , than to
650 solid fraction Φ (Agnolin and Roux 2007c; Magnanimo et al. 2008). z varies, between different
651 preparation procedures, independently of Φ for dense systems (Agnolin and Roux 2007a; Magnan-
652 imo et al. 2008). Of course, elastic moduli also reflect the anisotropy of the reference, prestressed
653 state, both due to stresses and to internal fabric. Anisotropic elastic properties have been probed
654 in experiments for some time (Hoque and Tatsuoka 1998; Kuwano and Jardine 2002; Duttine et al.
655 2007) and are currently being explored by numerical simulations (La Ragione and Magnanimo
656 2012a; La Ragione and Magnanimo 2012b).

657 The elastic behavior, albeit restricted to very small strain intervals, is an essential ingredient
658 in the discussion of incremental elastoplastic properties, the detailed form of which is important
659 for instability criteria. Elastic moduli also indirectly provide access, in a nondestructive way, to
660 geometrical data on the contact network, such as coordination number and fabric anisotropy.

661 **Granular plasticity**

662 Most micromechanical models are based on a relationship between force and relative displace-
663 ment vectors on contact planes or mobilized planes, and a dependence of the parameters on the

664 distribution of contact planes (Christoffersen et al. 1981; Chang and Hicher 2005; Chang et al.
665 2009; Chang et al. 2011). Such models are conceptually simple but capture the main features
666 of the stress-strain behavior in monotonic shearing. An important element of such models is the
667 relation between local and global strain or stress variables. A rational assumption is that the forces
668 on each contact plane are equal to the components of the stress tensor. This is obviously not
669 an exact assumption since the contact forces have a highly inhomogeneous distribution. Another
670 possible assumption is a kinematically constrained microstructure in which the local displacements
671 are components of the macroscopic strain tensor. This is equivalent to the assumption that the
672 velocity field has no non-affine components, which is wrong and leads to over-estimated predic-
673 tions for elastic moduli, for example (Kruyt and Rothenburg 2002a). Another constraint used in
674 micromechanical approach is the equality between energy dissipation rate $\sigma_{ij} \dot{\epsilon}_{ij}$ and frictional
675 dissipation at all sliding contacts (Cambou 1993). This is a strong assumption since only a small
676 proportion of contacts are critical and the friction forces have a broad distribution. Furthermore,
677 careful numerical simulations indicate that nearly 25% of energy dissipation in the quasi-static limit
678 is due to inelastic collisions between grains (Radjai and Roux 2004). This energy is dissipated by
679 micro-instabilities during shear and their signature on the critical-state shear stress can be observed
680 in the form of fluctuations.

681 The current challenge in micromechanics of granular materials is to account for fabric anisotropy
682 required for understanding and modeling complex loading paths (Wan and Guo 2004; Dafalias and
683 Manzari 2004; Li and Dafalias 2015; Radjai 2009; Sun and Sundaresan 2011; Radjai et al. 2012;
684 Chang and Bennett 2015). Because of the problems arising from a proper definition of grain-scale
685 kinematics from the boundary or far-field displacements via a localization tensor, there is presently
686 no general expression for the evolution of the coordination number, fabric tensor and dilatancy.
687 For this reason, most models consider only the effects of geometrical anisotropy by introducing,
688 for example, different elastic moduli for loading and unloading. It should be noted that in a
689 constitutive model developed on the basis of monotonic loading behavior or involving no tensorial
690 internal variable, the response upon unloading is elastic. In practice, however, a granular material
691 is “fragile” in the sense that stress increments in directions opposite to the shear directions cannot
692 be supported without plastic deformation (Cates et al. 1998). This leads to long plastic transients
693 when the direction of shearing is changed before the critical state is reached in the new direction

694 (Radjai and Roux 2004). If shear reversal is repeated at small strains, the system is attracted to a
695 new state that has not yet been investigated from a micromechanical viewpoint (Alonso-Marroquin
696 and Herrmann 2002). This state is a consequence of subtle memory effects that pull the packing
697 towards a high density but low coordination number.

698 **Origins of internal friction**

699 Frictional behavior is the most basic and common feature of the plasticity of granular materials.
700 In contrast to dry friction between two solid bodies, it is a bulk property. It has also been described
701 as friction between two “blocks” of a granular materials separated by a shear band. The localization
702 of shear deformation along a thin interface inside a dense granular material or with a structure is
703 an interesting analogy with dry friction between solid bodies but it masks the general properties
704 of granular friction and those of loose granular materials and steady flows, which cannot simply be
705 described by shear bands.

706 Granular friction reflects the collective motions of a large number of grains and it has a tensorial
707 nature. In particular, it is not a simple function of friction between grains. The internal (or global)
708 friction coefficient μ^* in steady flow (or in the critical state of soil mechanics) has a non-vanishing
709 value even for frictionless grains (Peyneau and Roux 2008b). The energy dissipation in this limit
710 results from inelastic collisions between grains and, since the collision velocity is proportional to
711 the mean effective stress p , it increases proportionally to p , as required by a Coulomb-like friction.
712 Furthermore, as the grain-grain friction coefficient μ_s increases, μ^* increases but it levels off for
713 $\mu_s \simeq 0.4$ (Taboada et al. 2006). Above this value, μ^* is independent of μ_s . The expression (8)
714 of stress tensor makes it possible to calculate from DEM simulations the contribution of friction
715 forces to the total shear stress and hence internal friction angle $\mu^* = \tan(\sigma_t/\sigma_n)$ along a granular
716 shear flow by considering only the tangential components f_t of forces. Quite unexpectedly, this
717 contribution is quite small (below 10%) (Thornton and Randall 1988).

718 Another quantity that is expected to correlate with internal friction coefficient is the proportion
719 of sliding contacts or critical contacts, i.e. contacts where friction is fully mobilized $f_t/f_n = \mu_s$.
720 For spherical grains, in the quasi-static state the proportion of sliding contacts is below 10%. In
721 a granular pile gradually tilted from horizontal to its maximum angle of stability, this proportion
722 increases exponentially towards its maximum value (Staron et al. 2002). The sliding points inside a

723 packing can be described as dislocations that carry plastic deformations. Their percolation across a
 724 packing eventually leads to failure. This viewpoint is interesting as it hints at avalanche precursors.
 725 But it does not provide a clear understanding of the properties of granular friction.

726 The above observations indicate that the bulk friction of granular materials is not a direct
 727 consequence of frictional contacts between grains but rather a *structural effect*. This was clearly
 728 established by a new partition of the stress tensor introduced by Rothenburg and Bathurst (Bathurst
 729 and Rothenburg 1988). The expression of stress tensor can be evaluated as an integral from the
 730 probability density function $P(\vec{f}, \vec{\ell})$ of branch vectors $\vec{\ell}$ (vectors joining grain centers) and contact
 731 forces \vec{f} . One needs also to introduce the angular distributions of contact normals $P(\vec{n})$ and force
 732 averages $f_n(\vec{n})$ and $f_t(\vec{n})$, where \vec{n} is the orientation of the branch vectors. In a sheared granular
 733 material, these functions can be approximated by their truncated Fourier expansions in 2D (or
 734 expansions in spherical harmonics in 3D):

$$735 \quad P(\theta) \simeq \frac{1}{\pi} \{1 + a_c \cos 2(\theta - \theta_c)\} \quad (10)$$

$$736 \quad \langle f_n \rangle(\theta) \simeq \langle f \rangle \{1 + a_n \cos 2(\theta - \theta_f)\} \quad (11)$$

$$737 \quad \langle f_t \rangle(\theta) \simeq \langle f \rangle a_t \sin 2(\theta - \theta_f) \quad (12)$$

738 where $\langle f \rangle$ is the average contact force, θ_c is the preferred direction of contacts and θ_f is the preferred
 739 direction of forces. The above expressions together with the integral expression of the stress tensor
 740 yield two relations (here in 2D) (Bathurst and Rothenburg 1988):

$$741 \quad p = n_c \langle f \rangle \langle \ell \rangle \quad (13)$$

$$742 \quad \frac{\sigma_1 - \sigma_3}{\sigma_1 + \sigma_3} = \sin \varphi = \frac{1}{2} (a_c + a_n + a_t) \quad (14)$$

743 where p is the mean effective pressure, $\langle \ell \rangle$ is the average branch vector length, φ is the internal
 744 friction angle, a_c is contact orientation anisotropy (fabric anisotropy), a_n is normal force anisotropy
 745 and a_t is tangential force anisotropy. The above expressions are obtained by assuming that the
 746 principal major direction θ_σ of the stress tensor is the same as θ_c and θ_f . This is a reasonable
 747 assumption since all directions tend to coincide during a monotonic shear deformation.

748 Equation (13) is similar to the perfect gas law with contacts playing the role of molecules

749 and $\langle f \rangle \langle \ell \rangle$ replacing $k_B T$, where k_B is the Boltzmann constant and T is absolute temperature.
750 Equation (14) is an explicit expression of the internal friction angle as a function of fabric and
751 force anisotropies. These two equations are in excellent agreement with simulations in monotonic
752 shear deformation. For unmonotonic deformations, the coaxiality of the branch vectors and forces
753 is not verified and hence it is necessary to account for the phase factors (Radjai and Richefeu 2009):

$$754 \quad \sin \varphi \simeq \frac{1}{2} \{ (a_c + a_\ell) \cos 2(\theta_\sigma - \theta_c) + (a_n + a_t) \cos 2(\theta_\sigma - \theta_f) \} \quad (15)$$

755 where the anisotropy a_ℓ of the branch vector length is also added and described by a truncated
756 Fourier expansion. This expression is nicely verified in simulations both in cohesive and noncohesive
757 materials, and under unmonotonic conditions. This indicates that the internal friction coefficient
758 has three distinct origins: 1) fabric anisotropy $a_c + a_\ell$, 2) normal force chains captured by a_n and 3)
759 friction mobilization quantified by a_t . The relation between a_t and friction mobilization is evident
760 by noting that, according to equation (12), the largest value of the ratio $\langle f_t \rangle / f$ occurs along the
761 direction $\theta = \theta_f + \pi/4$. Equation (15) clearly shows that friction mobilization is not the only factor
762 giving rise to the internal friction but that the contributions of force chains and contact network
763 anisotropy can even be more important.

764 The respective weights of the above anisotropies vary with particle size distribution (PSD) and
765 grain shapes. For example, in a packing of spherical grains the fabric anisotropy is above the
766 normal force anisotropy whereas in a packing of polyhedral grains the normal force anisotropy
767 is higher than fabric anisotropy (Azéma et al. 2009). This reflects the fact that force chains are
768 reinforced by face-face contacts between polyhedral grains. The fabric anisotropy a_c declines as
769 PSD becomes broader but branch vector length anisotropy a_ℓ increases (Voivret et al. 2009). The
770 force anisotropies remain unchanged since force chains are captured by the class of largest grains.
771 As a result, the internal friction angle remains nearly independent of PSD.

772 It is often assumed that the shear strength of granular materials increases with their compactness
773 measured in terms of their void ratio e and/or coordination number z . However, the compactness
774 does not explicitly appear in equation (15). Hence, the effect of compactness on the shear strength is
775 mediated by the fabric and force anisotropies. The steric exclusions in the close environments of the
776 grains imply that the maximum value of fabric anisotropy decreases as z increases, which seems to

777 be in contradiction with the increase of shear strength. The point is that the shear strength should
778 not be evaluated only from the actual state of the microstructure but from the potential hardening
779 of the material, which is clearly controlled by the evolution of the anisotropy. A material with high
780 value of z may loose more contacts along the direction of extension without being destabilized, hence
781 developing higher degree of anisotropy. This leads to a high peak strength. At still larger shear
782 deformation, contact gain in the direction of contraction increases and the anisotropy declines to
783 its critical-state value. In this way, the critical state is characterized by a detailed balance between
784 the gain and loss processes of contacts along and perpendicular to the direction of shear strain rate.

785 **RECENT DEVELOPMENTS IN MACROSCOPIC MODELING**

786 Alongside micromechanical approach, recent progress in macroscopic modeling has mainly fo-
787 cussed on the foundations of classical concepts and models of granular behavior. Among various
788 developments in this context, the authors will present below the thermo-mechanical consistency of
789 models, anisotropy as an independent parameter of the critical state, material instability, statistical
790 physics approach and inertial granular flows.

791 **Thermo-mechanical framework**

792 Most macroscopic models of granular behavior address correctly the material objectivity and
793 fit a group of experimental data. The objectivity, however, does not ensure the consistency of such
794 models with the framework of thermodynamics along all deformation paths. Indeed, while the
795 thermomechanics of materials has undergone significant developments (Ziegler and Wehrli 1987;
796 Maugin 1992), its application to granular materials is rather recent (Collins 1997; Collins and
797 Hilder 2002; Collins 2005). In this framework, the yield function, flow rule and hardening rules
798 of an elasto-plastic or a hypoplastic theory should be determined from the knowledge of the free
799 energy function A and a dissipation (or dissipation date) function Φ . The work increment is given
800 by $\delta W = \sigma_{ij} d\varepsilon_{ij} = dA + \delta\Phi$ with $\delta\Phi \geq 0$ in general, and $\delta\Phi > 0$ when plastic deformations occur.
801 Only A is a state function of elastic and plastic strains. The partial derivatives of A and $\delta\Phi$ with
802 respect to plastic deformations give rise to a back stress and dissipative stress, respectively.

803 The plastic dissipation is the product of the dissipative stress with the plastic strain increment
804 whereas shift stress dissipates no energy. The back stress is equivalent to kinematic hardening with
805 the displacement of the yield locus. Its physical origin as recoverable plastic work can be attributed

806 to “locked-in” elastic strains at the grains scale. This is also consistent with the observation that in
807 granular materials only a weak fraction of frictional contacts slip and dissipate energy (Radjai et al.
808 1998). More generally, it is suggested that the bimodal nature of stress transmission in granular
809 materials is consistent with this partition and can be used to construct general elasto-plastic models
810 with physical internal variables (Collins and Hilder 2002).

811 Collins and Hilder showed that most models, including the modified Cam Clay, do involve back
812 stresses and recoverable plastic work. They outlined a general method for the construction of the
813 yield function and flow rule. These laws are first formulated in terms of dissipative stresses with
814 associated flow rule. Then, they are transformed to the true stress space by adding the back stress.
815 This procedure is applied to introduce families of isotropic and anisotropic models which include
816 Mohr-Coulomb and Nor-sand models as special cases (Collins and Hilder 2002). The strength-
817 dilatancy relation is shown to be a consequence of the intimate relation between dilatancy and
818 anisotropy. One interesting feature of this energetic approach is that the flow rule arises from the
819 transformation between dissipative and true stress spaces without requiring a plastic potential.

820 **Accounting for anisotropy in constitutive modeling**

821 The generic anisotropy of granular texture has been a permanent source of inspiration for
822 improved modeling of granular behavior (Hoque and Tatsuoka 1998; Kruyt and Rothenburg 2004;
823 Dafalias and Manzari 2004; Wan and Guo 2004; Radjai and Roux 2004; Alonso-Marroquin et al.
824 2005; Li et al. 2012; Zhao and Guo 2013; Gao et al. 2014; Dafalias 2016). In particular, equation
825 (15) clearly shows that the stress ratio is nearly proportional to the contact anisotropy and a
826 phase factor that accounts for the difference between the privileged contact direction and major
827 principal stress direction. If the phase effect were absent, then contact anisotropy would simply be
828 a redundant parameter and could therefore be ignored in macroscopic modeling (the stress ratio
829 playing the same role as contact anisotropy). However, this not the case since for a granular texture
830 obtained along a strain path or through an arbitrary dynamic preparation method such as pouring
831 into a container, the stress state (magnitudes and directions) can change almost instantaneously,
832 and the transient deformations are then controlled by the evolution of the phase difference through
833 the fabric change. Furthermore, not only the stress ratio but also the dilatancy depend on loading
834 direction, a property that is ignored in the conventional CST (M et al. 1998).

835 In this way, the directional dependence of mechanical response raises a fundamental issue re-
 836 garding the definition of the CS, which is classically characterized by a critical value of the stress
 837 ratio η_c and a critical void ratio e_c (depending on the ratio of the average stress to a characteristic
 838 stress of the material) with no reference to loading direction compared to the fabric state. The
 839 issue is the ‘dimensionality’ of the critical domain in the state parameter space and its uniqueness
 840 (Radjai and Roux 2004; Radjai 2009; Li et al. 2012; Zhao and Guo 2013; Dafalias 2016). This
 841 point was recently addressed by a subtle Anisotropic Critical State Theory (ACST) (Li et al. 2012;
 842 Dafalias 2016). In this theory, the CS is characterized not only by the critical values of stress ratio
 843 and void ratio but also by a critical value of fabric anisotropy. Since dilatancy is the most signifi-
 844 cant parameter of the CST, the combined effect of loading direction and fabric state is formulated
 845 in terms of a Dilatancy State Line (DSL), parallel to the Critical State Line (CSL) on the (e, p)
 846 plane, which evolves towards the CSL as a function of a scalar anisotropy parameter reflecting the
 847 distance of the current fabric state to its critical state. On the other hand, the DSL replaces the
 848 CSL in its role of specifying the dilative or contractive state, depending on whether the current
 849 void ratio e is smaller or larger than the corresponding void ratio e_d at the same p . The new state
 850 parameter is defined by $\zeta = e - e_d = (e - e_c) - (e_d - e_c) = \psi - \psi_A$, where ψ is the usual state
 851 parameter and ψ_A represents the anisotropy of the model. The uniqueness and attainability of the
 852 CS is proved on the basis of the Gibbs condition of stability. The model is completed by a simple
 853 evolution equation for ψ_A , incorporating the requirement that the latter vanishes in the CS.

854 The ACST is a general framework within which various constitutive models may be formulated
 855 (Gao et al. 2014). It can be considered as a significant step beyond the CST with the advantage of
 856 shedding new light on the foundations of the CST and thus paving the way for further developments.
 857 The critical anisotropy may be evaluated from a grain-scale statistical approach. In particular, it can
 858 be shown that with an appropriate representation of local grain environments, the critical contact
 859 anisotropy a_c^* is related to the values of the coordination number z^{max} and z^{min} in the densest and
 860 loosest isotropic states, respectively, through a simple relation $a_c^* = 2(z^{max} - z^{min}) / (z^{max} + z^{min})$
 861 (Radjai 2009; Radjai et al. 2012).

Higher-order models

Most elastic-plastic models of granular behavior are *local* in the sense that the stress at each material point depends only on the strain or strain rate at the same point. Higher-order continuum models have been motivated by the finite size of shear bands, scale effects and particle rotations (Mulhaus and Vardoulakis 1987; Vardoulakis and Aifantis 1991; Vardoulakis and Sulem 1995). By introducing an internal length into the problem, such models remove the ill-posedness of the boundary-value problem arising in softening and shear localization. The internal length scale, which can be attributed either to grain size or the size of mesostructures, accounts for shear band thickness and allows for scale effects to be captured by the theory.

The internal length scales are definitely larger than single grain size (~ 10 grain diameters) as inferred from force-force correlations (see section 3). This force-related length reflects the correlations of the underlying texture and may thus partially depend on boundary conditions and fabric anisotropy, but it remains of the order of several grain diameters (Majmudar and Behringer 2005). However, non-affine velocities reveal much larger lengths involving correlated motions of particles (see section 3) (Radjai and Roux 2002). One highly nontrivial observation is the creeping of grains far away from a moving boundary (the so-called split-bottom geometry) (Nichol et al. 2010). Another well-documented observation is the decrease of the maximum angle of stability of a granular layer as a function of the thickness of the latter (Pouliquen 1999). Recently, S-shaped strain profiles were evidenced in experiments of plane shear flows indicating that the rheology is different close to the walls and its effects extends deeply into the medium (Miller et al. 2013). A local rheology predicts a linear profile when the stress state and all other fabric variables are constant across the flow. A more direct evidence for nonlocal behavior was provided by extensive simulations of Kuhn (Kuhn 2005). By imposing coerced nonuniform shearing, it was shown that the shear stress is strongly affected by both the first and second gradients of shear strain. The same simulations indicate that the dilatancy and particle rotations are not affected by gradients.

The gradient elastic-plastic models have been extensively worked out in the past (Vardoulakis and Aifantis 1991; Goddard 2014). They all involve only the second gradient on the basis that the first gradient is not compatible with the symmetry of the flow. A plastic material length ℓ_p is introduced as well as a reduced stress rate depending on the Laplacian of the plastic strain rate. The Laplacian accounts for the assumption that the behavior at a given point in the flow depends

892 on the nature of the flow in the surrounding region. Recently, Miller et al. used the concept
893 of granulence to introduce an eddy viscosity proportional to the imposed shear rate and squared
894 distance to the walls in order to estimate S-shaped velocity profiles (Miller et al. 2013). Another
895 successful nonlocal model is based on a state parameter field g called *granular fluidity* (Kamrin
896 and Koval 2012). It enters the rheology through its definition and $\dot{\gamma} = g\mu$ and its value at each
897 material point as a perturbation of its local value $g_{loc} = \dot{\gamma}_{loc}/\mu$ by its Laplacian $\xi^2\Delta g$ where ξ is a
898 cooperativity length proportional to grain size. This model has shown its ability to quantitatively
899 predict all the above-mentioned nonlocal effects (Kamrin and Henann 2015).

900 **Failure and instabilities**

901 Instability refers to a state of impossibility of quasi-static monotonic loading so that any in-
902 finitesimal load increment leads to dynamic evolution with a burst of kinetic energy or large de-
903 formations (Lade 2002; Nicot and Darve 2007). Experimental observations show that the failure is
904 either of geometrical nature as in column buckling, or of material origin as in constitutive behavior.
905 The latter has generally been associated either with vanishing of the determinant of the constitutive
906 tensor as precursor of homogeneous failure at the plastic limit or vanishing of the determinant of
907 the acoustic tensor with the emergence of plastic strain localization. These two criteria coincide
908 for an associative flow rule in which the elasto-plastic tensor is symmetric. But the non-associated
909 behavior of granular materials implies the loss of symmetry so that shear localization may occur
910 before the plastic limit.

911 Undrained triaxial tests on loose sand show a different type of failure at peak deviatoric stress
912 without shear localization (Nicot et al. 2007). The concepts of *controllability* and *sustainability* of
913 equilibrium states were introduced to account for this *diffuse failure*. Recently, from experiments
914 and DEM simulations it was shown that a whole bifurcation domain in the stress space exists with
915 various possible failure modes (Daouadji et al. 2011). The diffuse failure mode has a directional
916 character with respect to loading. The second-order work $d^2W = d\sigma_{ij}d\varepsilon_{ij}$ has been used to analyze
917 failure modes inside the plastic domain. This criterion includes both the plastic limit condition
918 and strain localization, which are special cases of the vanishing of second-order work. The micro-
919 instabilities are always present in sheared granular materials in the form of local bursts of individual
920 or collective inertial grain motions but they generally do not propagate to the macro-scale as a result

921 of disorder and energy dissipation. They propagate only when they are numerous and organized
922 in such a way that single grain motions are amplified by an avalanche-like process (Staron et al.
923 2002).

924 This means that a crucial step for a better understanding of failure is a detailed investigation
925 of the micro-transformations from the contact scale to the system scale, with due considerations
926 of sample size effects. Such processes can be studied, e.g., by deviator stress increments under
927 triaxial conditions. The general picture of the stress-strain behavior is a smooth process when
928 shear deformation is controlled. But when stress increments are applied, a granular material can
929 support finite stress increments without changes in the contact network (and without deformation
930 if grains are rigid) followed by fast rearrangements corresponding to a finite strain step (Combe
931 and Roux 2000; Roux and Combe 2002). With frictionless rigid grains, the finite strain jumps have
932 a Levy statistics, i.e. a power-law distribution of infinite mean – and no deterministic strain can
933 be associated to given stress increments, even in the large system limit (Combe and Roux 2000).
934 Dilatancy vanishes in such systems but a finite shear resistance is observed. Friction modifies
935 this distribution (Roux and Combe 2002), and smooth stress-strain curves are obtained for large
936 samples. The micro-instabilities by which contact networks rearrange and the fabric changes in
937 response to stress variations do not necessarily imply the existence of macro-instabilities (leading,
938 e.g., to strain localization). No specific study has been carried out yet, though, of the dependence of
939 the length scale associated to rearrangements on the proximity to a macroscopic instability criterion
940 except on sandpiles tilted from horizontal towards their angle of repose, indicating that a length
941 scale defined from friction mobilization increases and diverges as the maximum angle of stability is
942 approached (Staron et al. 2002; Staron and Radjai 2005).

943 **Statistical mechanics approach**

944 Besides kinetic theory of granular gases, an increasing number of researchers have dealt with
945 granular materials by means of concepts and theoretical tools of statistical mechanics. In such
946 attempts, granular media are very often used as a metaphor of amorphous materials such as colloids,
947 foams and glasses. For example, the SOC is a perfect model of out-of-equilibrium systems in which
948 sandpiles are used for illustration (Bak et al. 1988).

949 One of the earliest statistical models of granular matter is Edwards' volume ensemble (Edwards

950 and Oakeshott 1989). Since the volume (or packing fraction) of a granular material can change,
951 Edwards suggested that a microcanonical granular ensemble may be defined by all jammed mechan-
952 ically stable states of equal volume (replacing energy). Hence, a statistical mechanical model can be
953 built by assuming equiprobability of all such states. In particular, a “compactivity” variable can be
954 introduced as the derivative of the volume with respect to entropy (analogous to thermodynamical
955 temperature). There have been attempts to measure the volumetric entropy and compactivity of
956 simple granular systems from the distribution of volumes of tessellation cells (Aste and DiMatteo
957 2008). This has been further investigated by simulations and implies that the compactivity is a
958 measure of void ratio (Oquendo et al. 2016). A dual approach consists in considering the force
959 ensemble as the set of all force configurations with a given confining pressure (Snoeijer et al. 2004).

960 The statistical entropy has more generally been employed to rationalize force distributions and
961 local structures such as the distributions of coordination numbers, void valences and porosities (Bagi
962 1997; Kruyt and Rothenburg 2002b; Goddard 2004; Troadec et al. 2002; Aste et al. 2005; Kuhn
963 2014). Given a distribution P_i , maximizing the entropy $S = -\sum_i P_i \log P_i$ for a set of constraints
964 is equivalent to searching the most unbiased solution with respect to the missing information.
965 The results obtained by this method with a proper account of constraints are often in excellent
966 agreement with numerically simulated measures in the critical state for which meaningful statistics
967 can be extracted. But whether and why the critical state should be a maximally disordered state
968 (in the sense of the amount of missing information) is still a matter of discussion. One still needs
969 to show that the entropy is lower below and above the critical state.

970 Jamming transition, i.e. the arrest of particles from a dynamic state, has attracted considerable
971 work (Liu and Nagel 1998). A supercooled liquid turns into a glass with a finite yield stress as the
972 temperature is lowered. This process is very similar to the arrest of shaken grains in a packing of
973 finite yield stress when the shaking intensity is decreased or the packing fraction is lowered (Jaeger
974 2015). Such transitions may be described by the same jamming phase diagram with temperature,
975 packing fraction and pressure as control variables. Granular materials have been extensively used
976 as model system for the investigation of this *jamming diagram*.

977 Static disordered packings of spheres have been a subject of great interest for their geomet-
978 ric properties, which are relevant for all kinds of amorphous materials, made of atoms, colloidal
979 particles or macroscopic grains (Aste and Weaire. 2000; Aste et al. 2005; Torquato 2010). In

980 the absence of friction, rigid grains generically assemble under confining forces into configurations
981 devoid of force indeterminacy (i.e., given the geometry of the contact network, contact forces are
982 entirely determined by the external load and the equilibrium requirement). This sets upper bounds
983 on coordination numbers, which still apply to frictional grains. With spherical grains, isostaticity is
984 achieved (no displacement indeterminacy or “floppy mode” (Roux 2000; Torquato 2010) exists on
985 the force-contact network), which results in a coordination number equal to 6 if the “rattler” grains
986 that carry no force are excluded. Without friction, those configurations – often termed jammed in
987 the recent literature – are local minima of the potential energy of external forces (Roux 2000). If
988 subjected to an isotropic state of stress, they realize a local maximum of solid fraction in configura-
989 tion space – whence the identification (O’Hern et al. 2003; Agnolin and Roux 2007a) of the *random*
990 *close packing* (RCP) state with such isotropically confined assemblies of rigid frictionless objects,
991 provided it can be regarded as uniquely defined – all volume-minimizing configurations, if quickly
992 assembled, sharing the same solid fraction in the limit of large systems. This latter condition
993 appears to be satisfied for rapidly assembled packings (Agnolin and Roux 2007a), in which slow
994 evolutions (toward crystallization for identical beads) or, possibly, towards separation for mixtures,
995 do not take place (lack of uniqueness for slower protocols is shown in (Chaudhuri et al. 2010)).

996 The absence of dilatancy reported for frictionless objects (Peyneau and Roux 2008a; Azéma
997 et al. 2015) could partly explain that the same maximum density is recorded in various situations
998 of packings assembled quickly, but in such a way that the mobilization of friction is circumvented:
999 the stress state needs not be isotropic. The concept of the RCP, thus related to a mechanical
1000 definition, was however criticized as somewhat ill-defined by some authors (Torquato 2010), who
1001 adopted instead a notion of a Maximally Random Jammed (MRJ) packing of hard particles. The
1002 MRJ state minimizes some order metric under a condition of jamming. A discussion of jamming
1003 (stability of equilibrium state under the given external load) for arbitrary-shaped, frictional grains
1004 is provided in (Bagi 2007).

1005 **Inertial granular flows**

1006 Most modeling attempts mentioned above concern “quasi-static” deformations of granular ma-
1007 terials, which are assumed be rate-independent. However, the flow of granular matter is common
1008 in the transport of granular materials such as minerals and cereals, as well as at larger scales of

1009 rock avalanches, debris flows and other geological surface processes. Bagnold was the first to model
 1010 granular flows by considering grains of average size d and density ρ_s subjected to a controlled shear
 1011 flow of rate $\dot{\gamma}$ at constant volume. With these parameters, a dimensional analysis implies that
 1012 the shear stress τ is proportional to $\rho_s d^2 \dot{\gamma}^2$ with a prefactor depending on the packing fraction ϕ
 1013 (Bagnold 1954).

1014 For a long time, the scaling of shear stress as $\dot{\gamma}^2$ was considered to be a consequence of mo-
 1015 mentum exchange whose average value and frequency are proportional to the shear rate. This
 1016 scaling was incorporated in a general theory of “rapid granular flows” but its applicability to dense
 1017 granular flows remained questionable as most flows encountered in practice are both frictional and
 1018 collisional (Hutter and Scheiwiler 1983; Campbell 1990). The general theory of collisional granular
 1019 materials was developed using the classical formalism of kinetic theory and by introducing a *gran-*
 1020 *ular temperature* $T = \langle \delta v^2 \rangle$, the mean square of nonaffine (or fluctuating) particle velocities, and
 1021 by introducing a dissipation term through restitution coefficients for mass conservation (Jenkins
 1022 and Savage 1983). In this theory, all stresses are of kinetic origin. It should also be recalled that
 1023 reference physical system in both rapid flows and granular gases has been constant-volume shear
 1024 and the rheology is described by normal and shear viscosities η_n and η_t , respectively, defined by
 1025 $p = \eta_n \dot{\epsilon}_t$ and $\tau = \eta_t \dot{\epsilon}_t$, where $\dot{\epsilon}_t$ is the shear rate.

1026 It was only in 2004 that it became clear that frictional and inertial flows can be described in
 1027 the same framework if the volume as control parameter is replaced by the confining pressure p
 1028 (GDR-MiDi 2004). The relevant dimensionless number is then the inertial number I :

$$1029 \quad I = \dot{\gamma} d \left(\frac{\rho_s}{p} \right) \quad (16)$$

1030 This number is the ratio of the internal relaxation time of the grains $d(\rho_s/p)$ to the shear time $1/\dot{\gamma}$.
 1031 At low values of I , typically below 10^{-3} , the flow is rate-independent. At higher values of I , the bulk
 1032 friction coefficient μ increases with I whereas the packing fraction decreases. Phenomenological
 1033 laws $\mu(I)$ and $\phi(I)$ for steady granular flows in combination with continuum conservation equations
 1034 correctly predict the velocity and stress fields in various flow geometries (da Cruz et al. 2005; Jop
 1035 et al. 2006). The increase of μ with I despite an increasingly lower packing fraction reveals a
 1036 genuine microstructure. As I increases, the force chains become more sparse, the correlation length

1037 of connected particles decrease, the contact lifetimes decline, and an increasing number of impulsive
1038 forces and frictionally mobilized contacts come into play. Azema and Radjai applied stress partition,
1039 as in quasi-static deformations (see section 4), to show that the main mechanism for the increase
1040 of μ is contact anisotropy (Azéma and Radjai 2014).

1041 In the I -based rheology, $\mu(I)$ and $\phi(I)$ are the main variables. However, using the definition
1042 of I , it is straightforward to obtain the ϕ -based rheology (constant volume) with $\eta_n = I^{-2}$ and
1043 $\eta_t = \mu I^{-2}$. Using the data, it is shown that both viscosities diverge as $(\phi_c - \phi)^{-\alpha}$, with $\alpha \simeq 2$,
1044 when $I \rightarrow 0$, corresponding to $\phi \rightarrow \phi_c$ (Boyer et al. 2011). The value of ϕ_c is $\simeq 0.58$ for spherical
1045 particles of the same size and coincides with the CS packing fraction at low confining pressures.
1046 A similar divergence is observed in dense suspensions. This indicates that the same framework
1047 may be used to unify dense granular flows and dense viscous suspensions by accounting for viscous
1048 forces as well as inertial and frictional forces.

1049 **CONCLUSIONS: EXPANDING FRONTIERS**

1050 The fast expansion of granular science does not yet seem to converge to a common denominator.
1051 While new frontiers are constantly explored, there remain gaps and barriers that have been dodged
1052 or left for future. The developments have been driven by so many problems of practical interest,
1053 increasingly resolved measurements and imaging techniques, DEM simulations of increasing compu-
1054 tational efficiency and fruitful analogy with glassy materials. The simple packing of equal spheres
1055 has grown into a complex conceptual object in which the frontiers between trivial and fundamental
1056 are sometimes confused. But these are only signs of an explosive expansion of the field.

1057 Relating the macroscopic behavior of granular materials to their microstructure is a long-
1058 standing dream, which has not yet been realized. A long path remains towards a multiscale ap-
1059 proach based on the details of granular microstructure. For example, there is still only a partial
1060 understanding of relevant fabric variables and no general model for their evolution. Many models
1061 consider only simple loading paths in which a single scalar state parameter may just be enough.
1062 The role of mesoscale structures and their correlations also remain to be clarified. Advanced con-
1063 stitutive models can account for complex loading paths but their state variables are not explicitly
1064 connected with variables pertaining to the microstructure. On the other hand, the particle-scale
1065 variables such as forces and mobilized contacts have broad and scale-dependent distributions which

1066 are often well characterized from simulations and experiments but they elude statistical modeling.

1067 In the same way, despite decisive progress made on inertial granular flows, the empirical expres-
1068 sions of shear stress and packing fraction as a function of the inertial number have no theoretical
1069 basis. Although nonlocal effects have been evidenced by experiments and simulations and captured
1070 by models based on higher gradients of strain or a state parameter (as in the fluidity model), a
1071 pending question remains as to the nature of fluidity and some observations such as the dependence
1072 of the stress on the first strain gradient. It is important to note that the continuum equations as-
1073 sume a representative volume element. The nonlocal effects refer mostly to the grain size, which is
1074 clearly not a representative size of the material behavior. Moreover, the perturbations introduced
1075 by the boundary walls in the microstructure and their long-range correlations together with a local
1076 model thoroughly based on the microstructure may allow replacing nonlocal models to explain such
1077 “nonlocal” effects. These aspects clearly need further investigation.

1078 An important aspect of granular materials concerns particle geometrical properties such as their
1079 shape and size distributions. Such geometrical effects are crucial in many applications and they
1080 raise fundamental questions with respect to shear strength, dilatancy, stability and flow of granular
1081 materials. For example, the packing fraction is not a monotonous function of the particle shape
1082 as it deviates from a sphere; see Fig. 6. A generic shape parameter may be introduced to capture
1083 this effect of asphericity, but second-order shape parameters are also important for shear strength
1084 and space-filling properties of particles. This is a vast field that only begins to be investigated
1085 in a systematic fashion. The shape and size effects need enhanced experimental and numerical
1086 skills. The reason is that particle shapes cannot easily be controlled and numerical simulations
1087 require more advanced techniques of contact detection and much larger numbers of particles as size
1088 polydispersity and shape variability in samples increases.

1089 3D printing of particles opens the way for systematic experimental research along these lines.
1090 Particles of nonconvex and other exotic shapes can thus be produced. A packing of such particles
1091 is governed by real *interlocking* of the particles leading to a “geometric cohesion” (Franklin 2012).
1092 Star-shaped, Z-shaped and similar particles spontaneously jam in stable structures of high shear
1093 strength when poured into a container. Hence, optimizing particle shape may allow one to *design*
1094 structures that can emerge from random jamming of particles. This is what Jaeger calls “jamming
1095 by design” as a “process that gets us from desired properties to requirements for the constituent

1096 components” (Jaeger 2015; Reis et al. 2015). Packings of nonconvex aggregates of overlapping
1097 spheres can be optimized to create the densest packing (Roth and Jaeger 2016). This is not only
1098 of immense interest to the design of special microstructures in sintered powders combining high
1099 permeability, strength and manageability, for example, but also to the architecture and industrial
1100 design communities to create innovative structures.

1101 Besides particle geometry, there is presently a vast scope for research on several other aspects
1102 that were omitted from this review. The topic of cohesive granular materials and their flow behavior
1103 has been much less at the focus of recent research. Cohesive interactions may be due to solid surface
1104 forces as in fine powders or a consequence of capillary forces as in unsaturated soils. The mixing
1105 process of a powder with a liquid, distribution of liquid clusters, packing states and their rheology
1106 have only recently been investigated at the particle scale. The agglomeration process in applications
1107 to powders in food science and iron ores in steel-making industry is complex as it involves both
1108 cohesive interactions and inertial flows.

1109 Granular materials composed of crushable particles and their behavior while the particles can
1110 break under evolving load and/or deformation have been mostly investigated in connection with
1111 soils and rockfills. Particle breakage affects the stress-strain behavior as a result of the evolution of
1112 particle size distribution, which affects in turn the dilatancy and hence shear strength (Daouadji
1113 et al. 2001; Einav 2007; Russell et al. 2009; Daouadji and Hicher 2010). Other effects concern
1114 the evolution of particle shapes and their frictional contacts that induce nontrivial effects. Such
1115 evolving granular materials have often been modeled by assuming that each particle is an aggregate
1116 of smaller particles. However, to avoid finite size effects, it is necessary to consider larger aggregates
1117 and large packings of aggregates in order to be able to extract useful information from such discrete
1118 models.

1119 Another area of research, remaining almost fully unexplored, is that of ultra-soft particles. In
1120 hard granular materials, the elastic deformations are assumed to be concentrated at the contact
1121 points, and thus described as a function of the rigid-body degrees of freedom of the particles. This
1122 approximation is too crude in many applications, and the particles undergo large deformations
1123 (Nezamabadi et al. 2015). Metallic powders, for example, deform plastically without rupture.
1124 Likewise, many pharmaceutical and food products are soft-particle materials. The particle shape
1125 change occurs also in clays, which are composed of nano-scale aggregates. Such materials can

1126 undergo volume change by particle shape and size change under moderate external load with
1127 enhanced space filling properties. The compaction and shear behavior beyond this “jamming”
1128 limit require fundamental research effort in the future. Proper simulation methods, by coupling a
1129 continuum description of the particles, with the Material Point Method that can allow for large
1130 deformations, for example, coupled with contact dynamics method for the treatment of contacts
1131 between deformable particles, need to be developed.

1132 Although only the modeling aspects were at the focus of this paper, let us recall here that the re-
1133 search on granular materials has been developed from increasingly precise experimental techniques
1134 to measure particle displacement fields and forces (Lesniewska and Wood 2009). The development
1135 of new measurement techniques and their applications to various granular experiments can be a
1136 subject of a stand-alone review paper. Automated simultaneous measurements of applied stresses
1137 and strains in arbitrary directions are already in use in soil mechanics. The experimental challenge
1138 has been so far the perfect control of boundary conditions and homogeneity of samples. However,
1139 the challenge has now shifted to the measurement of fabric variables in 3D packings of particles
1140 by resolving contacts between particles. Today, high-resolution X-ray computed tomography can
1141 provide access to this information (Andò et al. 2012). 3D photoelastic imaging of forces is cur-
1142 rently being developed (Brodu et al. 2015), and it will be a valuable tool for accessing normal
1143 and tangential forces and their evolution. The ultimate experiment for future will be simultaneous
1144 measurements of particle displacements and contact forces in 3D with variable boundary conditions.

1145
1146 The authors thank Mahdi Taeibat for fruitful discussions. Farhang Radjai would like to ac-
1147 knowledge the support of the ICoME2 Labex (ANR-11-LABX-0053) and the A*MIDEX projects
1148 (ANR-11-IDEX-0001-02) cofunded by the French program Investissements d’Avenir, managed by
1149 the French National Research Agency (ANR).

APPENDIX I. REFERENCES

- 1150
- 1151 Agnolin, I. and Roux, J.-N. (2007a). “Internal states of model isotropic granular packings. I. As-
- 1152 sembling process, geometry, and contact networks..” *Phys Rev E*, 76(6-1), 061302.
- 1153 Agnolin, I. and Roux, J.-N. (2007b). “Internal states of model isotropic granular packings. II.
- 1154 Compression and pressure cycles..” *Phys Rev E*, 76(6-1), 061303.
- 1155 Agnolin, I. and Roux, J.-N. (2007c). “Internal states of model isotropic granular packings. III.
- 1156 Elastic properties..” *Phys Rev E*, 76(6-1), 061304.
- 1157 Alonso-Marroquin, F. and Herrmann, H. J. (2002). “Calculation of the incremental stress-strain
- 1158 relation of a polygonal packing.” *Phys. Rev. E*, 66(2), 021301–.
- 1159 Alonso-Marroquin, F., Luding, S., Herrmann, H. J., and Vardoulakis, I. (2005). “Role of anisotropy
- 1160 in the elastoplastic response of a polygonal packing.” *Phys. Rev. E*, 71(5), 051304.
- 1161 Andò, E., Hall, S. A., Viggiani, G., Desrues, J., and Bésuelle, P. (2012). “Experimental microme-
- 1162 chanics: grain-scale observation of sand deformation.” *Géotechnique Letters*, 2, 107–112.
- 1163 Andrade, J., Avila, C., Hall, S., Lenoir, N., and Viggiani, G. (2011). “Multiscale modeling and
- 1164 characterization of granular matter: From grain kinematics to continuum mechanics.” *Journal*
- 1165 *of the Mechanics and Physics of Solids*, 59, 237–250.
- 1166 Andrade, J. E. and Tu, X. (2009). “Multiscale framework for behavior prediction in granular media.”
- 1167 *Mechanics of Materials*, 41, 652–669.
- 1168 Antony, S. J. (2001). “Evolution of force distribution in three-dimensional granular media..” *Phys.*
- 1169 *Rev. E*, 63(1 Pt 1), 011302.
- 1170 Aste, T. and DiMatteo, T. (2008). “Emergence of gamma distributions in granular materials and
- 1171 packing models.” *Phys. Rev. E*, 77, 021309.
- 1172 Aste, T., Saadatfar, M., and Senden, T. J. (2005). “The geometrical structure of disordered sphere
- 1173 packings.” *Phys. Rev. E*, 71, 061302.
- 1174 Aste, T. and Weaire., D. (2000). *The Pursuit of Perfect Packing*. Institute of Physics Publishing.
- 1175 Azéma, E. and Radjai, F. (2014). “Internal structure of inertial granular flows.” *Phys. Rev. Lett.*,
- 1176 112(7), 078001–.
- 1177 Azéma, E., Radjai, F., Peyroux, R., and Saussine, G. (2007). “Force transmission in a packing of
- 1178 pentagonal particles..” *Phys. Rev. E*, 76(1 Pt 1), 011301.

1179 Azéma, E., Radjai, F., and Roux, J.-N. (2015). “Internal friction and absence of dilatancy of
1180 packings of frictionless polygons.” *Phys. Rev. E*, 91, 010202(R).

1181 Azema, E., Radjai, F., Saint-Cyr, B., Delenne, J.-Y., and Sornay, P. (2013). “Rheology of 3d
1182 packings of aggregates: microstructure and effects of nonconvexity.” *Phys. Rev. E*, 87, 052205.

1183 Azéma, E., Saussine, G., and Radjai, F. (2009). “Quasistatic rheology, force transmission and fabric
1184 properties of a packing of irregular polyhedral particles.” *Mechanics of Materials*, 41, 729–741.

1185 Bagi, K. (1997). “Analysis of micro-variables through entropy principle.” *Powders and Grains 1997*,
1186 R. Behringer and J. T. Jenkins, eds., Balkema, Rotterdam, 251–254.

1187 Bagi, K. (2007). “On the Concept of Jammed Configurations from a Structural Mechanics Perspec-
1188 tive.” *Granular Matter*, 9, 109–134.

1189 Bagnold, R. A. (1954). “Experiments on a gravity-free dispersion of large solid spheres in a newto-
1190 nian fluid under shear.” *Proc. Royal Soc. London*, 225, 49–63.

1191 Bak, P., Tang, C., and Wiesenfeld, K. (1987). “Self-organized criticality: An explanation of $1/f$
1192 noise.” *Phys. Rev. Lett.*, 59(4), 381–384.

1193 Bak, P., Tang, C., and Wiesenfeld, K. (1988). “Self-organized criticality.” *Phys. Rev. A*, 38(1),
1194 364–375.

1195 Bardet, J. P. (1994). “Observations on the effects of particle rotations on the failure of idealized
1196 granular materials.” *Mechanics of Materials*, 18, 159–182.

1197 Bathurst, R. J. and Rothenburg, L. (1988). “Micromechanical aspects of isotropic granular assem-
1198 blies with linear contact interactions.” *J. Appl. Mech.*, 55, 17.

1199 Been, K. and Jefferies, M. (1985). “A state parameter for sands.” *Géotechnique*, 35, 99–112.

1200 Bernal, J. D. (1960). “Geometry and the structure of monatomic liquids.” *Nature*, 185, 68–70.

1201 Berryman, J. G. (1986). “Random close packing of hard spheres and disks.” *Phys. Rev. A*, 27, 1053.

1202 Biarez, J. (1962). “Contribution à l’étude des propriétés mécaniques des sols et des matériaux
1203 pulvérulents.” Ph.D. thesis, Grenoble, France, Grenoble, France.

1204 Bolton, M. D. (1986). “The strength and dilatancy of sands.” *Géotechnique*, 36, 65–78.

1205 Boyer, F., Guazzelli, E., and Pouliquen, O. (2011). “Unifying suspension and granular rheology.”
1206 *Phys. Rev. Lett.*, 107, 18.

1207 Brodu, N., Dijkstra, J. A., and Behringer, R. P. (2015). “Spanning the scales of granular materials
1208 through microscopic force imaging.” *Nature Communications*, 6:6361.

1209 Cambou, B. (1993). “From global to local variables in granular materials.” *Powders and Grains*
1210 *93*, C. Thornton, ed., Amsterdam, A. A. Balkema, 73–86.

1211 Campbell, C. S. (1990). “Rapid granular flows.” *Annu. Rev. Fluid Mech.*, *22*, 57.

1212 Casagrande, A. (1936). “Characteristics of cohesionless soils affecting the stability of slopes and
1213 earth fills.” *J. Boston Soc. Civil Eng.*, *23*, 257–276.

1214 Cates, M. E., Wittmer, J. P., Bouchaud, J.-P., and Claudin, P. (1998). “Jamming, force chains,
1215 and fragile matter.” *Phys. Rev. Lett.*, *81*(9), 1841–1844.

1216 Chang, C. S. and Bennett, K. (2015). “Micromechanical modeling for the deformation of sand
1217 with noncoaxiality between the stress and material axes.” *Journal of Engineering Mechanics*,
1218 C4015001.

1219 Chang, C. S. and Hicher, P.-Y. (2005). “An elasto-plastic model for granular materials with mi-
1220 crostructural consideration.” *International Journal of Solids and Structures*, *42*, 4258–4277.

1221 Chang, C. S., Hicher, P. Y., and Daouadji, A. (2009). “Investigating instability in granular ma-
1222 terials by means of a micro-structural model.” *European Journal of Environmental and Civil*
1223 *Engineering*, *13*, 167–186.

1224 Chang, C. S. and Misra, A. (1990). “Application of uniform strain theory to heterogeneous granular
1225 solids.” *Journal of Engineering Mechanics*, *116*, 2310–2328.

1226 Chang, C. S., Yin, Z.-Y., and Hicher, P.-Y. (2011). “Micromechanical analysis for interparticle and
1227 assembly instability of sand.” *Journal of Engineering Mechanics*, *137*, 155–168.

1228 Chaudhuri, P., Berthier, L., and Sastry, S. (2010). “Jamming Transitions in Amorphous Packings
1229 of Frictionless Spheres Occur over a Continuous Range of Volume Fractions.” *Phys. Rev. Lett.*,
1230 *104*(16).

1231 Christoffersen, J., Mehrabadi, M. M., and Nemat-Nasser, S. (1981). “A micromechanical description
1232 of granular material behavior.” *J. Appl. Mech.*, *48*, 339–344.

1233 Collins, I. F. (1997). “The use of legendre transformations in developing the constitutive laws of
1234 geomechanics from thermodynamic principles.” *IUTAM Symposium on Mechanics of Granular*
1235 *and Porous Materials*, N. A. Fleck and A. C. E. Cocks, eds., Kluwer Academic Publishers, 151–
1236 159.

1237 Collins, I. F. (2005). “Elastic/plastic models for soils and sands.” *International Journal of Mechan-*
1238 *ical Sciences*, *47*(4-5), 493–508.

1239 Collins, I. F. and Hilder, T. (2002). “A theoretical framework for constructing elastic/plastic con-
1240 stitutive models of triaxial tests.” *Int. J. Numer. Anal. Meth. Geomech.*, 26, 1313–1347.

1241 Combe, G., Richefeu, V., and Stasiak, M. (2015). “Experimental validation of a nonextensive scaling
1242 law in confined granular media.” *Phys. Rev. Lett.*, 115, 238301.

1243 Combe, G. and Roux, J.-N. (2000). “Strain versus stress in a model granular material: A devil’s
1244 staircase.” *Phys. Rev. Lett.*, 85(17), 3628–3631.

1245 Coppersmith, S. N., Liu, C., Majumdar, S., Narayan, O., and Witten, T. A. (1996). “Model for
1246 force fluctuations in bead packs.” *Phys. Rev. E*, 53(5), 4673–4685.

1247 Coulomb, C. A. (1773). “Essai sur un application de règles de maximis et minimis à quelques
1248 problèmes de staique relatifs à l’architcture.” *Acad. R. Sci. Mem. Math. Phys. Acad. R. Sci.*,
1249 *Paris*, 7, 343–382.

1250 Coulomb, C. A. (1781). “Théorie des Machines Simples.” *Academie des Sciences*, 10, 166.

1251 Coumoulos, D. G. (1967). *A radiographic study of soils*. University of Cambridge.

1252 Cundall, P. A. and Strack, O. D. L. (1979). “A discrete numerical model for granular assemblies.”
1253 *Géotechnique*, 29(1), 47–65.

1254 Cundall, P. A. and Strack, O. D. L. (1983). “Modeling of microscopic mechanisms in granular
1255 materials.” *Mechanics of Granular Materials: New Models and Constitutive Relations*, J. T.
1256 Jenkins and M. Satake, eds., Amsterdam, Elsevier, 137–149.

1257 da Cruz, F., Emam, S., Prochnow, M., Roux, J.-N., and cois Chevoir, F. (2005). “Rheophysics of
1258 dense granular materials: discrete simulation of plane shear flows.” *Phys. Rev. E*, 72(2 Pt 1),
1259 021309.

1260 Dafalias, Y. (2016). “Must critical state theory be revisited to include fabric effects?.” *Acta Geotech-*
1261 *nica*, 11, 479–491.

1262 Dafalias, Y. F. and Manzari, M. T. (2004). “Simple plasticity sand model accounting for fabric
1263 change effects.” *Journal of Engineering Mechanics*, 130, 622–634.

1264 Dantu, P. (1957). “Contribution à l’étude mécanique et géométrique des milieux pulvérulents.”
1265 *Proc. Of the 4th International Conf. On Soil Mech. and Foundation Eng.*, Vol. 1, London, But-
1266 terworths Scientific Publications, 144–148.

1267 Daouadji, A., Darve, F., Gali, H. A., Hicher, P. Y., Laouafa, F., Lignon, S., Nicot, F., Nova, R.,
1268 Pinheiro, M., Prunier, F., Sibille, L., and Wan, R. (2011). “Diffuse failure in geomaterials: Ex-

1269 periments, theory and modelling.” *International Journal for Numerical and Analytical Methods*
1270 *in Geomechanics*, 35, 1731–1773.

1271 Daouadji, A. and Hicher, P. Y. (2010). “An enhanced constitutive model for crushable granular
1272 materials.” *Int. J. Num. Anal. Methods in Geomechanics*, 34, 555–580.

1273 Daouadji, A., Hicher, P. Y., and Rahma, A. (2001). “Modelling grain breakage influence on me-
1274 chanical behaviour of granular media.” *European Journal of Mechanics, A/solids*, 20, 113–137.

1275 Darve, F. and Laouafa, F. (1999). “Plane strain instabilities in soil: Application to slopes instabil-
1276 ity.” *Numerical Models in Geomaterials*, Prande, Pietruszczak, and Schweiger, eds., Rotterdam,
1277 Balkema, 85–90.

1278 Darwin, G. H. (1883). “On the horizontal thrust of a mass of sand.” *Minutes of the Proceedings*
1279 *Institution of Civil Engineering*, 350–378.

1280 Desrues, J., Lanier, J., and Stutz, P. (1983). “Localization of deformation in tests on sand samples.”
1281 *Eng. Fracture Mechanics*, 21, p909–921.

1282 Desrues, J., Chambon, R., Mokni, M., and Mazerolles, F. (1996). “Void ratio evolution inside shear
1283 band in triaxial sand specimens studied by computed tomography.” *Géotechnique*, 46, 529–546.

1284 Donev, A., Cisse, I., Sachs, D., Variano, E. A., Stillinger, F. H., Connelly, R., Torquato, S., and
1285 Chaikin, P. M. (2004). “Improving the density of jammed disordered packings using ellipsoids..”
1286 *Science*, 303(5660), 990–993.

1287 Donev, A., Torquato, S., and Stillinger, F. H. (2005). “Pair correlation function characteristics
1288 of nearly jammed disordered and ordered hard-sphere packings..” *Phys Rev E Stat Nonlin Soft*
1289 *Matter Phys*, 71(1 Pt 1), 011105.

1290 Drescher, A. and de Josselin de Jong, G. (1972). “Photoelastic verification of a mechanical model
1291 for the flow of a granular material.” *J. Mech. Phys. Solids*, 20, 337–351.

1292 Duttine, A., Di Benedetto, H., Pham Van Bang, D., and Ezaoui, A. (2007). “Anisotropic small
1293 strain elastic properties of sands and mixture of sand-clay measured by dynamic and static
1294 methods.” *Soils and Foundations*, 47(3), 457–472.

1295 E., B. (1996). “Calibration of a comprehensive constitutive equation for granular material.” *Soils*
1296 *Found.*, 36, 13–26.

1297 Edwards, S. F. and Oakeshott, R. B. S. (1989). “Theory of powders.” *Physica A*, 157, 1080.

1298 Einav, I. (2007). “Breakage mechanics, part i: theory.” *Journal of the Mechanics and Physics of*

1299 *Solids*, 55, 1274–1297.

1300 Einav, I. (2012). “The unification of hypo-plastic and elasto-plastic theories.” *International Journal*
1301 *of Solids and Structures*, 49, 1305–1315.

1302 Estrada, N., Taboada, A., and Radjai, F. (2008). “Shear strength and force transmission in granular
1303 media with rolling resistance.” *Phys. Rev. E*, 78.

1304 Franklin, S. V. (2012). “Geometric cohesion in granular materials.” *Physics Today*.

1305 Fuentes, W., Triantafyllidis, T., and Lizcano, A. (2012). “Hypoplastic model for sands with loading
1306 surface.” *Acta Geotechnica*, 7, 177–192.

1307 Gao, Z., Zhao, J., Li, X.-S., and Dafalias, Y. F. (2014). “A critical state sand plasticity model
1308 accounting for fabric evolution.” *Int. J. Numer. Anal. Meth. Geomech.*, 38, 370–390.

1309 GDR-MiDi (2004). “On dense granular flows.” *Eur. Phys. J. E*, 14, 341–365.

1310 Geoffroy, H., di Benedetto, H., Duttine, A., and Sauzéat, C. (2003). “Dynamic and cyclic loadings
1311 on sands: results and modelling for general stress-strain conditions.” *Deformation characteristics*
1312 *of geomaterials*, H. diBenedetto, T. Doanh, H. Geoffroy, and C. Sauzéat, eds., Lisse, Swets and
1313 Zeitlinger, 353–363.

1314 Goddard, J. (2004). “On entropy estimates of contact forces in static granular assemblies.” *Inter-*
1315 *national Journal of Solids and Structures*, 41(21), 5851–5861.

1316 Goddard, J. (2014). “Continuum modeling of granular media.” *Applied Mechanics Reviews*, 66,
1317 050801.

1318 Goddard, J. D. (1990a). “Nonlinear elasticity and pressure-dependent wave speeds in granular
1319 media.” *Proc. R. Soc. Lond. A*, 430, 105.

1320 Goddard, J. D. (1990b). “Nonlinear elasticity and pressure-dependent wave speeds in granular
1321 media.” *Proc. Roy. Soc. London*, 430, 105–131.

1322 Goldhirsch, I. and Zanetti, G. (1993). “Clustering instability in dissipative gases.” *Phys. Rev. Lett.*,
1323 70(11), 1619–1622.

1324 Grammenoudis, P. and Tsakmakis, C. (2005). “Finite element implementation of large deformation
1325 micropolar plasticity exhibiting isotropic and kinematic hardening effects.” *Numerical Methods*
1326 *in Engineering*, 62, 1691–1720.

1327 Gudehus, G. S. F. (1996). “A comprehensive constitutive equation for granular materials.” *Soils*
1328 *Found.*, 36, 1–12.

1329 Guo, N. and Zhao, J. (2016). “Parallel hierarchical multiscale modelling of hydro-mechanical prob-
1330 lems for saturated granular soils.” *Comput. Methods Appl. Mech. Engrg.*, 305, 37–61.

1331 Hashiguchi, K. (1979). “A derivation of the associated flow rule.” *J. Fac Agric. Kyushu Univ.*, 24,
1332 75–80.

1333 Hashiguchi, K. and Chen, Z. P. (1998). “Elastoplastic constitutive equation of soils with the subload-
1334 ing surface.” *Int. J. Numer. Anal. Methods Geomech.*, 22, 197–227.

1335 He, Q. C. (2014). “On the micromechanical definition of macroscopic strain and strain-rate tensors
1336 for granular materials.” *Computational Materials Science*, 94, 51–57.

1337 Hicher, P.-Y. (1996). “Elastic properties of soils.” *ASCE Journal of Geotechnical Engineering*, 122,
1338 641–648.

1339 Hoque, E. and Tatsuoka, F. (1998). “Anisotropy in elastic deformation of granular materials.” *Soils
1340 and Foundations*, 38, 163–179.

1341 Huang, W., Sloan, S., and Fityus, S. (2008). “Incorporating a predefined limit condition in a
1342 hypoplastic model by means of stress transformation.” *Mechanics of Materials*, 40, 796–802.

1343 Huang, W.-X., Wu, W., Sun, D.-A., and Sloan, S. (2006). “A simple hypoplastic model for normally
1344 consolidated clay.” *Acta Geotechnica*, 1, 15–27.

1345 Hutter, K. and Scheiwiler, T. (1983). “Rapid plane flow of granular materials down a chute.”
1346 *Mechanics of granular media – New models and constitutive relations*, Amsterdam, Elsevier.

1347 Jaeger, H. and Nagel, S. (1996). “Granular solids, liquids and gases.” *Reviews of Modern Physics*,
1348 68, 1259–1273.

1349 Jaeger, H. M. (2015). “Celebrating soft matter’s 10th anniversary: Toward jamming by design.”
1350 *Soft Matter*, 11, 12–27.

1351 Jaeger, H. M., Liu, C., Nagel, S. R., and Witten, T. A. (1990). “Flow in granular materials:
1352 Self-organized non-critical behavior.” *Relaxation and Related Topics in Complex Systems*, A.
1353 Campbell and C. Giovannella, eds., Plenum Press, London, 235.

1354 Jefferies, M. G. (1993). “Nor-sand : a simple critical state model for sand.” *Géotechnique*, 43,
1355 91–103.

1356 Jefferies, M. G. and Been, K. (2006). *Soil Liquefaction: A Critical State Approach*. Taylor & Francis,
1357 London.

1358 Jenkins, J. T. and Richman, M. W. (1985). “Kinetic theory for plane flows of a dense gas of

1359 identical, rough, inelastic, circular disks.” *Phys. of Fluids*, 28, 3485–3494.

1360 Jenkins, J. T. and Savage, S. B. (1983). “A theory for the rapid flow of identical, smooth, nearly
1361 elastic, spherical particles.” *J. Fluid Mech.*, 130, 187–202.

1362 Jia, X., Caroli, C., and Velický, B. (1999). “Ultrasound propagation in externally stressed granular
1363 media.” *Phys. Rev. Lett.*, 82, 1863–1866.

1364 Johnson, K. L. (1985). *Contact Mechanics*. Cambridge University Press.

1365 Jop, P., Forterre, Y., and Pouliquen, O. (2006). “A constitutive law for dense granular flows..”
1366 *Nature*, 441(7094), 727–730.

1367 Jullien, R., Meakin, P., and Pavlovitch, A. (1992). “Random packings of spheres built with sequen-
1368 tial models.” *J. of Phys. A*, 25, 4103.

1369 Kamrin, K. and Henann, D. L. (2015). “Nonlocal modeling of granular flows down inclines.” *Soft
1370 Matter*, 2015, 11, 179–185.

1371 Kamrin, K. and Koval, G. (2012). “Nonlocal constitutive relation for steady granular flow.” *Phys.
1372 Rev. Lett.*, 108, 178301.

1373 Kaneko, K., Terada, K., Kyoya, T., and Kishino, Y. (2003). “Global-local analysis of granular media
1374 in quasi-static equilibrium.” *International Journal of Solids and Structures*, 40, 4043–4069.

1375 Katagiri, J., Matsushima, T., and Yamada, Y. (2010). “Simple shear simulation of 3d irregularly-
1376 shaped particles by image-based dem.” *Granular Matter*, 12, 491–497.

1377 Kolymbas, D. (1991). “An outline of hypoplasticity.” *Arch. App. Mech.*, 61, 143–154.

1378 Kolymbas, D., Herle, I., and von Wolfersdorff, P. A. (1995). “Hypoplastic constitutive equa-
1379 tion with internal variables.” *Int. J. for Numerical and Analytical Methods in Geomechanics*,
1380 19(XXX), 415–436.

1381 Kruyt, N. P. and Rothenburg, L. (1996). “Micromechanical definition of strain tensor for granular
1382 materials.” *ASME Journal of Applied Mechanics*, 118, 706–711.

1383 Kruyt, N. P. and Rothenburg, L. (2002a). “Micromechanical bounds for the effective elastic moduli
1384 of granular materials.” *International Journal of Solids and Structures*, 39, 311–324.

1385 Kruyt, N. P. and Rothenburg, L. (2002b). “Probability density functions of contact forces for
1386 cohesionless frictional granular materials.” *International Journal of Solids & Structures*, 39, 571–
1387 583.

1388 Kruyt, N. P. and Rothenburg, L. (2004). “Kinematic and static assumptions for homogenization in

1389 micromechanics of granular materials.” *Mechanics of Materials*, 36(12), 1157–1173.

1390 Kuhn, M. R. (1999). “Structured deformation in granular materials.” *Mech. Mater.*, 31, 407–429.

1391 Kuhn, M. R. (2005). “Are granular materials simple? an experimental study of strain gradient
1392 effects and localization.” *Mechanics of Materials*, 37, 607–627.

1393 Kuhn, M. R. (2014). “Dense granular flow at the critical state: maximum entropy and topological
1394 disorder.” *Granular Matter*, 16, 499–508.

1395 Kuhn, M. R. and Bagi, K. (2004). “Contact rolling and deformation in granular media.” *Interna-
1396 tional Journal of Solids and Structures*, 41, 5793–5820.

1397 Kuwano, R. and Jardine, R. J. (2002). “On the applicability of cross-anisotropic elasticity to gran-
1398 ular materials at very small strains.” *Géotechnique*, 52, 727–749.

1399 La Ragione, L. and Jenkins, J. T. (2007). “The initial response of an idealised granular material.”
1400 *Proceedings of the Royal Society A*, 463, 735–758.

1401 La Ragione, L. and Magnanimo, V. (2012a). “Contact anisotropy and coordination number for
1402 a granular assembly: A comparison of distinct-element-method simulations and theory.” *Phys.
1403 Rev. E*, 031304.

1404 La Ragione, L. and Magnanimo, V. (2012b). “Evolution of the effective moduli of an anisotropic,
1405 dense, granular material.” *Granular Matter*, 14, 749–757.

1406 Lade, P. V. (1994). “Instability and liquefaction of granular materials.” *Computers and Geotechnics*,
1407 16, 123–151.

1408 Lade, P. V. (2002). “Instability, shear banding, and failure in granular materials.” *International
1409 Journal of Solids and Structures*, 39, 3337–3357.

1410 Lanier, J., Caillerie, D., Chambonn, R., Viggiani, G., Blesuelle, P., and Desrues, J. (2004). “A
1411 general formulation of hypoplasticity.” *Int. J. Numer. Anal. Meth. Geomech.*, 28, 1461–1478.

1412 Lesniewska, D. and Wood, D. M. (2009). “Observations of stresses and strains in a granular mate-
1413 rial.” *Journal of Engineering Mechanics*, 135, 1038–1054.

1414 Li, X. and Dafalias, Y. (2000). “Dilatancy for cohesionless soils.” *Geotechnique*, 50, 449–460.

1415 Li, X. and Dafalias, Y. (2015). “Dissipation consistent fabric tensor definition from dem to contin-
1416 uum for granular media.” *Journal of the Mechanics and Physics of Solids*, 78, 141–153.

1417 Li, X. S., , and Dafalias, Y. F. (2012). “Anisotropic critical state theory: Role of fabric.” *J. Eng.
1418 Mech.*, 138, 263–275.

1419 Liu, A. J. and Nagel, S. R. (1998). “Jamming is not just cool any more.” *Nature*, 396, 21–22.

1420 Liu, C. (1994). “Spatial patterns of sound propagation in sand.” *Phys. Rev. B*, 50.

1421 Liu, C. and Nagel, S. R. (1992). “Sound in sand.” *Phys. Rev. Lett.*, 68(15), 2301–2304.

1422 Liu, C. and Nagel, S. R. (1994). “Sound and vibration in granular materials.” *J. Phys.: Condens.*
1423 *Matter*, 6, A433–A436.

1424 Liu, C., Nagel, S. R., Schecter, D. A., Coppersmith, S. N., Majumdar, S., Narayan, O., and Witten,
1425 T. A. (1995). “Force fluctuations in bead packs.” *Science*, 269, 513.

1426 Liu, Y., Sun, W., Yuan, Z., and Fish, J. (2016). “A nonlocal multiscale discrete-continuum model
1427 for predicting mechanical behavior of granular materials.” *Int. J. Numer. Meth. Engng*, 106,
1428 129–160.

1429 Love, A. (1929). *A Treatise of the Mathematical Theory of Elasticity*. Cambridge University Pres.

1430 M, Y., K, I., and W, V. (1998). “Effects of principal stress direction and intermediate principal
1431 stress on undrained shear behavior of san.” *Soils Found*, 38, 179–188.

1432 Magnanimo, V., La Ragione, L., Jenkins, J. T., Wang, P., and Makse, H. A. (2008). “Characterizing
1433 the shear and bulk moduli of an idealized granular material.” *Europ. Phys. Lett.*, 81, 34006.

1434 Majmudar, T. and Behringer, R. (2005). “Contact force measurements and stress-induced
1435 anisotropy in granular materials.” *Nature*, 435, 1079–1082.

1436 Makse, H. A., Gland, N., Johnson, D., and Schwartz, L. (1999). “Why effective medium theory
1437 fails in granular materials.” *Phys. Rev. Lett.*, 83(24), 5070–5073.

1438 Makse, H. A., Johnson, D. L., and Schwartz, L. M. (2000). “Packing of compressible granular
1439 materials.” *Phys. Rev. Lett.*, 84(18), 4160–4163.

1440 Manzari, M. T. and Dafalias, Y. F. (1997). “A critical state two-surface plasticity model for sands.”
1441 *Géotechnique*, 47, 255–272.

1442 Masin, D. (2012). “Hypoplastic cam-clay model.” *Géotechnique*, 62, 549–553.

1443 Maugin, G. A. (1992). *The Thermomechanics of Plasticity and Fracture*. Cambridge University
1444 Press, Cambridge.

1445 McNamara, S. and Young, W. R. (1992). “Inelastic collapse and clumping in a one-dimensional
1446 granular medium.” *Phys. Fluids A*, 4(3), 496.

1447 McNamara, S. and Young, W. R. (1994). “Inelastic collapse in two dimensions.” *Phys. Rev. E*,
1448 50(1), R28–R31.

1449 Mehrabadi, M. M. and Cowin, S. C. (1978). “Initial planar deformation of dilatant granular mate-
1450 rials.” *J. Mech. Phys. Solids*, 26, 269–284.

1451 Metzger, P. T. (2004a). “Comment on ”mechanical analog of temperature for the description of
1452 force distribution in static granular packings”..” *Phys Rev E Stat Nonlin Soft Matter Phys*, 69(5
1453 Pt 1), 053301; discussion 053302.

1454 Metzger, P. T. (2004b). “Granular contact force density of states and entropy in a modified edwards
1455 ensemble..” *Phys Rev E Stat Nonlin Soft Matter Phys*, 70(5 Pt 1), 051303.

1456 Miller, B., O’Hern, C., and Behringer, R. P. (1996). “Stress fluctuations for continously sheared
1457 granular materials.” *Phys. Rev. Lett.*, 77, 3110–3113.

1458 Miller, T., Rognon, P., Metzger, B., and Einav, I. (2013). “Eddy viscosity in dense granular flows.”
1459 *Phys. Rev. Lett.*, 111, 058002.

1460 Mitchell, J. K. and Soga, K. (2005). *Fundamentals of Soil Behavior, third edition*. Wiley.

1461 Moreau, J. J. (1993). “New computation methods in granular dynamics.” *Powders & Grains 93*,
1462 Rotterdam, A. A. Balkema, 227.

1463 Mroz, Z., Norris, V. A., and Zienkiewicz, O. C. (1978). “An anisotropic hardening model for soils
1464 and its application to cyclic loading.” *Int. J. Numer. Anal. Methods Geomech.*, 2, 203–221.

1465 Mueth, D. M., Jaeger, H. M., and Nagel, S. R. (1998). “Force distribution in a granular medium.”
1466 *Phys. Rev. E*, 57, 3164.

1467 Mulhaus, H. B. and Vardoulakis, I. (1987). “The thickness of shear bands in granular materials.”
1468 *Géotechnique*, 37, 271–283.

1469 Nemat-Nasser, S., Mehrabadi, M. M., and Iwakuma, T. (1981). *Three Dimensional Constitutive*
1470 *Relations and Ductile Fractures*. North Holland, Amsterdam, Chapter On certain microscopic
1471 and macroscopic aspect of plastic flow of ductile material, 157–172.

1472 Newland, P. L. and Allely, B. H. (1957). “Volume changes in drained taixial tests on granular
1473 materials.” *Géotechnique*, 7, 17–34.

1474 Nezamabadi, S., Radjai, F., Averseng, J., and Delenne, J.-Y. (2015). “Implicit frictional contact
1475 model for soft particle systems.” *Journal of the Mechanics and Physics of Solids*, 83, 72–87.

1476 Nguyen, D.-H., Azéma, E., Radjai, F., and Sornay, P. (2014). “Effect of size polydispersity versus
1477 particle shape in dense granular media.” *Physical Review E*, 90(1), 012202.

1478 Nichol, K., Zanin, A., Bastien, R., Wandersman, E., and van Hecke, M. (2010). “Flow-induced

1479 agitations create a granular fluid.” *Phys. Rev. Lett.*, 104, 078302.

1480 Nicot, F. and Darve, F. (2007). “A micro-mechanical investigation of bifurcation.” *International*
1481 *Journal of Solids and Structures*, 44, 6630–6652.

1482 Nicot, F., Darve, F., and Khoa, H. (2007). “Bifurcation, second order-work in granular materials.”
1483 *International Journal for Numerical and Analytical Methods in Geomechanics*, 31, 1007–1032.

1484 Nitka, M., Combe, G., Dascalu, C., and Desrues, J. (2011). “Two-scale modeling of granular
1485 materials: a dem-fem approach.” *Granular Matter*, 13, 277–281.

1486 Noll, W. (1955). “Die herleitung der grundgleichungen der thermomechanik der kontinua aus der
1487 statistischen mechanik.” *J. Natural Mech. and Anal.*, XXX(4), 627–646.

1488 Noll, W. (1958). “A mathematical theory of the mechanical behavior of continuous media.” *Arch.*
1489 *Ration. Mech. Anal.*, 2, 197–226.

1490 Nova, R. (1982). *Soil Mech. - transient Cycl. Load.* Wiley, Chichester, Chapter A constitutive model
1491 for soil under monotonic and cyclic loading, 343–373.

1492 Nova, R. (1994). “Controllability of the incremental response of soil specimens subjected to arbitrary
1493 loading programmes.” *Journal of the Mechanical Behavior of Materials*, 5, 193–201.

1494 Oda, M. (1972). “Initial fabrics and their relations to mechanical properties of granular material.”
1495 *Soils and foundations*, 12, 17–36.

1496 Oda, M., Iwashita, K., and Kakiuchi, T. (1997). “Importance of particle rotation in the mechanics
1497 of granular materials.” *Powders & Grains 1997*, R. P. Behringer and J. T. Jenkins, eds., A. A.
1498 Balkema, Rotterdam, Netherlands, 207–210.

1499 Oda, M., Konishi, J., and Nemat-Nasser, S. (1982). “Experimental micromechanical evaluation of
1500 strength of granular materials: effects of particle rolling.” *Mechanics of Materials*, 1, 269–283.

1501 Oda, M., Koshini, J., and Nemat-Nasser, S. (1980). “Some experimentally based fundamental
1502 results on the mechanical behavior of granular materials.” *Geotechnique*, 30, 479–495.

1503 O’Hern, C., Langer, S., Liu, A., and Nagel, S. (2001). “Force distributions near jamming and glass
1504 transitions.” *Phys. Rev. Lett.*, 86(1), 111–114.

1505 O’Hern, C., Silbert, L. E., Liu, A. J., and Nagel, S. R. (2003). “Jamming at zero temperature and
1506 zero applied stress: The epitome of disorder.” *Physical Review E*, 68(1), 011306.

1507 Oquendo, W. F., Munoz, J. D., and Radjai, F. (2016). “An equation of state for granular media at
1508 the limit state of isotropic compression.” *EPL*, 114, 14004.

1509 Ouadfel, H. and Rothenburg, L. (2001). “Stress-force-fabric relationship for assemblies of ellipsoids.”
1510 *Mechanics of Materials*, 33(4), 201–221.

1511 Pavlovitch, A., Jullien, R., and Meakin, P. (1991). “Geometrical properties of a random packing of
1512 hard spheres.” *Physica A*, 176, 206.

1513 Peters, J. and Walizer, L. (2013). “Patterned non-affine motion in granular media.” *Journal of*
1514 *Engineering Mechanics*, 139, 1479–1490.

1515 Peyneau, P.-E. and Roux, J.-N. (2008a). “Frictionless bead packs have macroscopic friction, but
1516 no dilatancy.” *Physical Review E*, 78.

1517 Peyneau, P.-E. and Roux, J.-N. (2008b). “Solidlike behavior and anisotropy in rigid frictionless
1518 bead assemblies.” *Physical Review E*, 78.

1519 Pouliquen, O. (1999). “Scaling laws in granular flows down rough inclined planes.” *Phys. Fluids*,
1520 11(3), 542–548.

1521 Pouya, M. and Wan, R. (2016). “Strain in granular media: probabilistic approach to dirichlet
1522 tessellation.” *Journal of Engineering Mechanics*.

1523 Radjai, F. (2009). “Force and fabric states in granular media.” *Powders and Grains 2009*, N.
1524 Masami and S. Luding, eds., AIP, New York, 35–42.

1525 Radjai, F. (2015). “Modeling force transmission in granular materials.” *Comptes Rendus Physique*,
1526 16, 3–9.

1527 Radjai, F., Delenne, J.-Y., Azema, É., and Roux, S. (2012). “Fabric evolution and accessible
1528 geometrical states in granular materials.” *Granular Matter*, 14(2), 259–264.

1529 Radjai, F., Jean, M., Moreau, J.-J., and Roux, S. (1996). “Force distributions in dense two-
1530 dimensional granular systems.” *Phys. Rev. Lett.*, 77(2), 274–.

1531 Radjai, F. and Richefeu, V. (2009). “Bond anisotropy and cohesion of wet granular materials.”
1532 *Phil. Trans. R. Soc. A*, 367, 5123–5138.

1533 Radjai, F. and Roux, S. (2002). “Turbulentlike fluctuations in quasistatic flow of granular media..”
1534 *Phys Rev Lett*, 89(6), 064302.

1535 Radjai, F. and Roux, S. (2004). “Contact dynamics study of 2d granular media : Critical states
1536 and relevant internal variables.” *The Physics of Granular Media*, H. Hinrichsen and D. E. Wolf,
1537 eds., Weinheim, Wiley-VCH, 165–186.

1538 Radjai, F., Roux, S., and Moreau, J. J. (1999). “Contact forces in a granular packing..” *Chaos*,

1539 9(3), 544–550.

1540 Radjai, F., Troadec, H., and Roux, S. (2004). “Key features of granular plasticity.” *Granular*
1541 *Materials: Fundamentals and Applications*, S. Antony, W. Hoyle, and Y. Ding, eds., Cambridge,
1542 R.S.C, 157–184.

1543 Radjai, F. and Wolf, D. E. (1998). “The origin of static pressure in dense granular media.” *Granular*
1544 *Matter*, 1, 3–8.

1545 Radjai, F., Wolf, D. E., Jean, M., and Moreau, J. (1998). “Bimodal character of stress transmission
1546 in granular packings.” *Phys. Rev. Letter*, 80, 61–64.

1547 Reis, P. M., Jaeger, H. M., and van Hecke, M. (2015). “Designer matter: A perspective.” *Extreme*
1548 *Mechanics Letters*, 5, 25–29.

1549 Reynolds, O. (1885). “On the dilatancy of media composed of rigid particles in contact.” *Philos.*
1550 *Mag. Ser. 5*, 50-20, 469.

1551 Roscoe, K. H. (1970). “Tenth rankine lecture: The influence of strains in soil mechanics.”
1552 *Géotechnique*, 20, 129–170.

1553 Roscoe, K. H. and Schofield, A. N. (1963). “Mechanical behaviour of an idealised wet clay.” *2nd*
1554 *Eur. Conf. Soil Mech. Found. Eng. Wiesbaden*, 47–54.

1555 Roscoe, K. H., Schofield, A. N., and Wroth, C. P. (1958). “On the yielding of soils.” *Géotechnique*,
1556 8, 22–53.

1557 Roth, L. K. and Jaeger, H. M. (2016). “Optimizing packing fraction in granular media composed
1558 of overlapping spheres.” *Soft Matter*, 12, 1107–1115.

1559 Rothenburg, L. and Bathurst, R. J. (1989). “Analytical study of induced anisotropy in idealized
1560 granular materials.” *Geotechnique*, 39, 601–614.

1561 Roux, J.-N. (2000). “Geometric origin of mechanical properties of granular materials.” *Phys. Rev.*
1562 *E.*, 61, 6802–6836.

1563 Roux, J.-N. and Combe, G. (2002). “Quasistatic rheology and the origins of strain.” *C. R. Physique*,
1564 3, 131–140.

1565 Roux, S. and Radjai, F. (2001). “Statistical approach to the mechanical behavior of granular media.”
1566 *Mechanics for a New Millennium*, H. Aref and J. Philips, eds., Netherlands, Kluwer Acad. Pub.,
1567 181–196.

1568 Rowe, P. W. (1962). “The stress-dilatancy relation for static equilibrium of an assembly of particles

1569 i contact.” *Proc. R. Soc. A Math. Phys. Eng. Sci. The Royal Societ*, 500–527.

1570 Russell, A. R., Wood, D. M., and Kikumoto, M. (2009). “Crushing of particles in idealized granular
1571 assemblies.” *J. Mech. Phys. Solids*, 57, 1293–1313.

1572 Saint-Cyr, B., Delenne, J.-Y., Voivret, C., Radjai, F., and Sornay, P. (2011). “Rheology of granular
1573 materials composed of nonconvex particles.” *Phys. Rev. E*, 84(4), 041302–.

1574 Satake, M. (1982). “Fabric tensor in granular materials.” *Proceedings of the IUTAM symposium
1575 on deformation and failure of granular materials, Delft*, P. A. Vermeer and H. J. Luger, eds.,
1576 Amsterdam, A. A. Balkema, 63–68.

1577 Schofield, A. N. and Wroth, P. (1968). *Critical State Soil Mechanics*. McGraw-Hill, London.

1578 Shibuya, S., Tatsuoka, F., Teachavorasinskun, S., Kong, X.-J., Abe, F., Kim, Y.-S., and Park, C.-S.
1579 (1992). “Elastic deformation properties of geomaterials.” *Soils and Foundations*, 32, 26–46.

1580 Silbert, L. E., Ertas, D., Grest, G. S., Halsey, T. C., and Levine, D. (2002). “Geometry of frictionless
1581 and frictional sphere packings.” *Phys; Rev. E*, 65(3), 031304.

1582 Snoeijer, J. H., Vlugt, T. J. H., van Hecke, M., and van Saarloos, W. (2004). “Force network
1583 ensemble: a new approach to static granular matter..” *Phys. Rev. Lett.*, 92(5), 054302.

1584 Somfai, E., Roux, J.-N., Snoeijer, J. H., van Hecke, M., and van Saarloos, W. (2005). “Elastic wave
1585 propagation in confined granular systems.” *Phys. Rev. E*, 72, 021301.

1586 Somfai, E., van Hecke, M., Ellenbroek, W. G., Shundyak, K., and van Saarloos, W. (2007). “Critical
1587 and noncritical jamming of frictional grains.” *Phys. Rev. E*, 75(2), 020301.

1588 Staron, L. and Radjai, F. (2005). “Friction versus texture at the approach of a granular avalanche..”
1589 *Phys Rev E*, 72(4 Pt 1), 041308.

1590 Staron, L., Radjai, F., and Vilotte, J.-P. (2005). “Multi-scale analysis of the stress state in a
1591 granular slope in transition to failure..” *Eur Phys J E Soft Matter*, 18(3), 311–320.

1592 Staron, L., Vilotte, J.-P., and Radjai, F. (2002). “Preavalanche instabilities in a granular pile.”
1593 *Phys. Rev. Lett.*, 89, 204302.

1594 Sun, J. and Sundaresan, S. (2011). “A constitutive model with microstructure evolution for flow of
1595 rate-independent granular materials.” *J. Fluid Mech.*, 682, 590–616.

1596 Taboada, A., Estrada, N., and Radjaï, F. (2006). “Additive decomposition of shear strength in
1597 cohesive granular media from grain-scale interactions..” *Phys. Rev. Lett.*, 97(9), 098302.

1598 Taiebat, M. and Dafalias, Y. F. (2008). “Sanisand: Simple anisotropic sand plasticity model.” *Int.*

1599 *J. Numer. Anal. Meth. Geomech.*, 32, 915–948.

1600 Taylor, D. W. (1948). *Fundamentals of soil mechanics*. Wiley, New York.

1601 Tejchman, J. and Wu, W. (1993). “Numerical study on patterning of shear bands in a cosserat
1602 continuum.” *Acta Mechanica*, 99, 61–74.

1603 Terzaghi, K. (1943). *Theoretical soil mechanics*. J. Wiley, New York.

1604 Thomann, T. G. and Hryciw, R. D. (1990). “Laboratory measurement of small strain shear modulus
1605 under k_0 conditions.” *ASTM Geotechnical Testing Journal*, 13(2), 97–105.

1606 Thornton, C. (1997). “Force transmission in granular media.” *KONA Powder and Particle*, 15,
1607 81–90.

1608 Thornton, C. and Randall, C. W. (1988). “Applications of theoretical contact mechanics to solid
1609 particle system simulation.” *Micromechanics of granular media*, Amsterdam, Elsevier.

1610 Tordesillas, A. (2007). “Force chain buckling, unjamming transitions and shear banding in dense
1611 granular assemblies.” *Philosophical Magazine*, 87(32), 4987–5016.

1612 Torquato, S. (2010). “Jammed hard-particle packings: From kepler to bernal and beyond.” *Reviews
1613 of Modern Physics*, 82, 2633–2672.

1614 Troadec, H., Radjai, F., Roux, S., and Charmet, J. (2002). “Model for granular texture with steric
1615 exclusion.” *Physical Review E*, 66(4 1), 041305–1.

1616 Vardoulakis, I. (1979). “Bifurcation analysis of the triaxial test on sand samples.” *Acta Mechanica*,
1617 32, 35–54.

1618 Vardoulakis, I. and Aifantis, E. C. (1991). “A gradient flow theory of plasticity for granular
1619 materials.” *Acta. Mech.*, 87, 197–217.

1620 Vardoulakis, I. and Sulem, J. (1995). *Bifurcation analysis in geomechanics*. Chapman & Hall, London.

1621 Verdugo, R. and Ishihara, K. (1996). “The steady state of sandy soils.” *Soils Found.*, 36, 81–91.

1622 Vermeer, P. A. (1998). “Non-associated plasticity for soils, concrete and rock.” *Physics of Dry
1623 Granular Media*, H. J. Herrmann, J.-P. Hovi, and S. Luding, eds., Dordrecht, Balkema, 163–196.

1624 Voivret, C., Radjai, F., Delenne, J.-Y., and Youssoufi, M. E. (2009). “Force transmission in poly-
1625 disperse granular media.” *Phys. Rev. Lett.*, 102, 178001.

1626 Walton, K. (1987). “The effective elastic moduli of a random packing of spheres.” *Journal of
1627 Mechanics and Physics of Solids*, 35, 213–226.

1628 Walton, O. R. and Braun, R. L. (1986). “Viscosity, granular temperature, and stress calculations

1629 for shearing assemblies of inelastic, frictional disks.” *J. Rheol.*, 30, 949.

1630 Wan, R. and Guo, P. (2004). “Stress dilatancy and fabric dependencies on sand behavior.” *Journal*
1631 *of Engineering Mechanics*, 130, 635–645.

1632 Wood, D. (1990). *Soil behaviour and critical state soil mechanics*. Cambridge University Press,
1633 Cambridge, England.

1634 Wu, W. (1998). “Rational approach to anisotropy of sand.” *Int. J. Numer. Anal. Meth. Geomech.*,
1635 22, 921–940.

1636 Wu, W. and Niemunis, A. (1996). “Failure criterion, flow rule and dissipation function derived from
1637 hypoplasticity.” *Mech. Cohesive-Frict. Mater.*, 1, 145–163.

1638 Wyart, M. (2006). “On the rigidity of amorphous solids.” *Annales de Physique Fr.*, 30, 1–96.

1639 Wyart, M., Nagel, S. R., and Witten, T. A. (2005). “Geometric origin of excess low-frequency
1640 vibrational modes in weakly connected amorphous solids.” *Europhysics Letters*, 72, 486–492.

1641 Zhao, J. and Guo, N. (2013). “Unique critical state characteristics in granular media considering
1642 fabric anisotropy.” *Géotechnique*, 63, 695–704.

1643 Zhu, H., Mehrabadi, M. M., and Massoudi, M. (2006). “Incorporating the effects of fabric in
1644 the dilatant double shearing model for planar deformation of granular materials.” *International*
1645 *Journal of Plasticity*, 22, 628–653.

1646 Ziegler, H. and Wehrli, C. (1987). “The derivation of constitutive relations from the free energy
1647 and the dissipation function.” *Advances in Applied Mechanics*, 25, 183–238.

1648

List of Figures

1649 1 Evolution of stress ratio (a) and packing fraction (b) as a function of cumulative
1650 plastic shear strain ε in DEM simulation of a packing of disks at constant confining
1651 pressure. Here, $q_n = 0.5(\sigma_1 - \sigma_2) \cos 2(\theta_\sigma - \theta_0)$ and $p = 0.5(\sigma_1 + \sigma_2)$, where σ_1 and
1652 σ_2 are the principal stresses and θ_σ and θ_0 are the principal stress direction and flow
1653 direction, respectively. The initial state is prepared by isotropic compaction. Note
1654 the long transient and unmonotonic evolution of packing fraction upon shear reversal. 59

1655 2 (a) The contact geometry; (b) First-shell particle environment with angular exclu-
1656 sions; (c) A loop of touching particles. 60

1657 3 (a) A map of normal forces in a polydisperse packing of disks. Line thickness is
1658 proportional to normal force; (b) A map of nonaffine particle displacements in a
1659 sheared packing of disks. 61

1660 4 Relevant scales in granular materials: contact, particle, assembly (microstructure),
1661 representative volume element (RVE) and macrostructure. 62

1662 5 Shear modulus G versus confining pressure P in different types of numerically simu-
1663 lated, isotropically compressed glass bead assemblies, denoted as A (crosses, contin-
1664 uous line), B (asterisks, dotted line), C (square dots, continuous line) and D (open
1665 squares, dotted line). Corresponding solid fractions Φ and coordination numbers z
1666 satisfy $\Phi_A \simeq \Phi_C > \Phi_B > \Phi_D$, and $z_A > z_B > z_C \simeq z_D$. The dashed line marked
1667 “KJ” corresponds to experimental data (Kuwano and Jardine 2002) on loose bead
1668 packs between 50 and 400 kPa. 63

1669 6 The packing fraction of an assembly of nonconvex aggregates each composed of three
1670 overlapping disks as a function of the degree of nonconvexity η 64

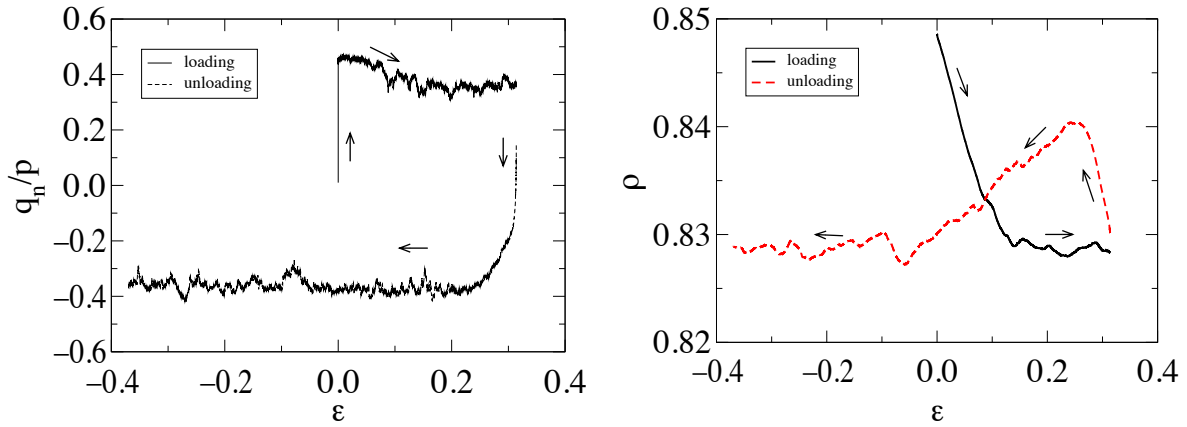


FIG. 1. Evolution of stress ratio (a) and packing fraction (b) as a function of cumulative plastic shear strain ε in DEM simulation of a packing of disks at constant confining pressure. Here, $q_n = 0.5(\sigma_1 - \sigma_2) \cos 2(\theta_\sigma - \theta_0)$ and $p = 0.5(\sigma_1 + \sigma_2)$, where σ_1 and σ_2 are the principal stresses and θ_σ and θ_0 are the principal stress direction and flow direction, respectively. The initial state is prepared by isotropic compaction. Note the long transient and unmonotonic evolution of packing fraction upon shear reversal.

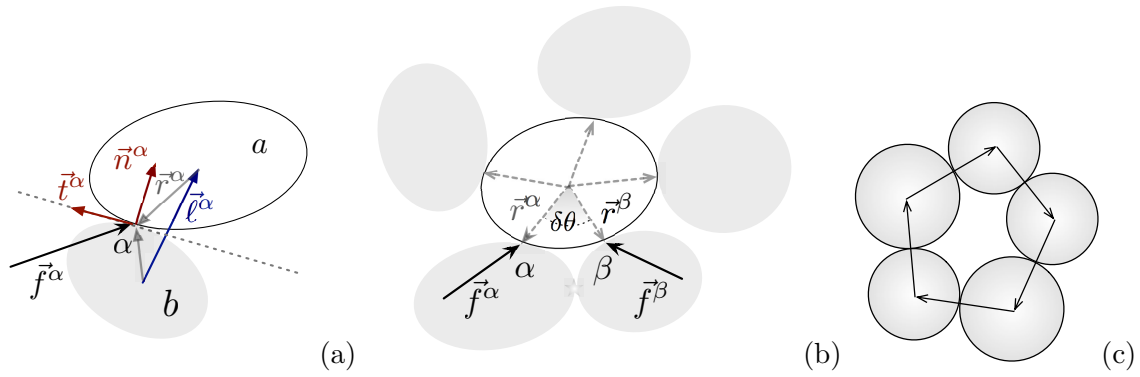
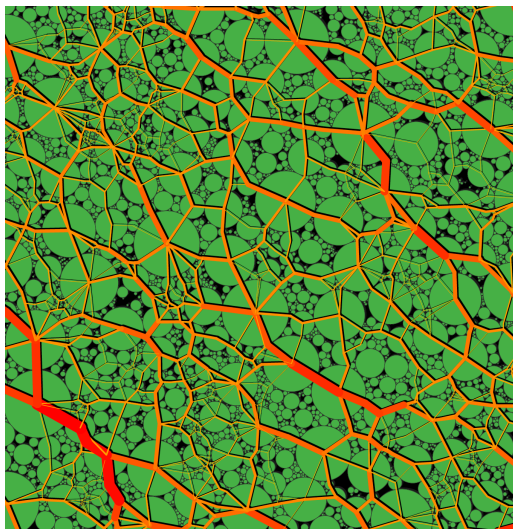
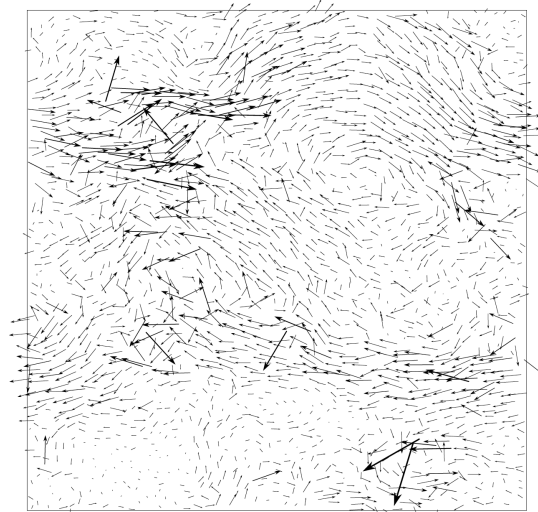


FIG. 2. (a) The contact geometry; (b) First-shell particle environment with angular exclusions; (c) A loop of touching particles.



(a)



(b)

FIG. 3. (a) A map of normal forces in a polydisperse packing of disks. Line thickness is proportional to normal force; (b) A map of nonaffine particle displacements in a sheared packing of disks.

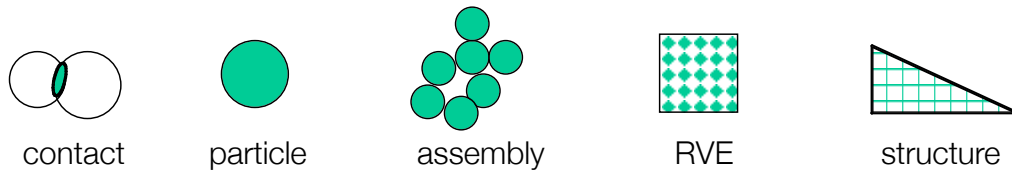


FIG. 4. Relevant scales in granular materials: contact, particle, assembly (microstructure), representative volume element (RVE) and macrostructure.

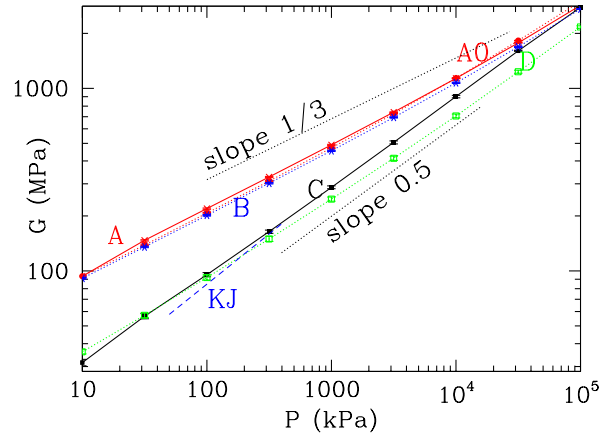


FIG. 5. Shear modulus G versus confining pressure P in different types of numerically simulated, isotropically compressed glass bead assemblies, denoted as A (crosses, continuous line), B (asterisks, dotted line), C (square dots, continuous line) and D (open squares, dotted line). Corresponding solid fractions Φ and coordination numbers z satisfy $\Phi_A \simeq \Phi_C > \Phi_B > \Phi_D$, and $z_A > z_B > z_C \simeq z_D$. The dashed line marked “KJ” corresponds to experimental data (Kuwano and Jardine 2002) on loose bead packs between 50 and 400 kPa.

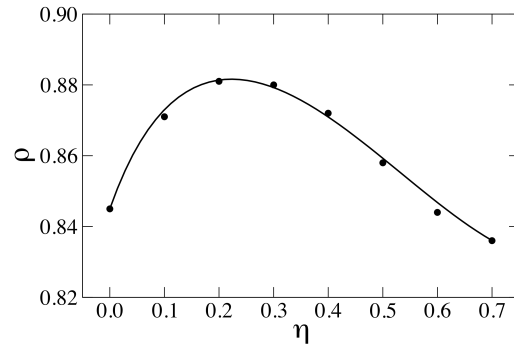


FIG. 6. The packing fraction of an assembly of nonconvex aggregates each composed of three overlapping disks as a function of the degree of nonconvexity η .